HHS Public Access

Author manuscript

Abdom Radiol (NY). Author manuscript; available in PMC 2021 March 12.

Published in final edited form as:

Abdom Radiol (NY). 2020 November ; 45(11): 3444–3462. doi:10.1007/s00261-020-02656-7.

MR elastography of liver: current status and future perspectives

Ilkay S. Idilman[1,2], **Jiahui Li**[1], **Meng Yin**[1], **Sudhakar K. Venkatesh**[1]

[1]Department of Radiology, Mayo Clinic Alix College of Medicine, Mayo Clinic, Rochester, MN, USA

[2]Department of Radiology, School of Medicine, Hacettepe University, Ankara, Turkey

Abstract

Non-invasive evaluation of liver fibrosis has evolved over the last couple of decades. Currently, elastography techniques are the most widely used non-invasive methods for clinical evaluation of chronic liver disease (CLD). MR elastography (MRE) of the liver has been used in the clinical practice for nearly a decade and continues to be widely accepted for detection and staging of liver fibrosis. With MRE, one can directly visualize propagating shear waves through the liver and an inversion algorithm in the scanner automatically converts the shear wave properties into an elastogram (stiffness map) on which liver stiffness can be calculated. The commonly used MRE method, two-dimensional gradient recalled echo (2D-GRE) sequence has produced excellent results in the evaluation of liver fibrosis in CLD from various etiologies and newer clinical indications continue to emerge. Advances in MRE technique, including 3D MRE, automated liver elasticity calculation, improvements in shear wave delivery and patient experience, are promising to provide a faster and more reliable MRE of liver. Innovations, including evaluation of mechanical parameters, such as loss modulus, displacement, and volumetric strain, are promising for comprehensive evaluation of CLD as well as understanding pathophysiology, and in differentiating various etiologies of CLD. In this review, the current status of the MRE of liver in CLD are outlined and followed by a brief description of advanced techniques and innovations in MRE of liver.

Keywords

Liver fibrosis; Elasticity; Viscosity; Damping ratio; Volumetric strain; 3D MRE

Introduction

Chronic liver injury by any etiology results in inflammation and destruction of hepatocytes, and the liver parenchyma responds by regeneration and fibrosis [1, 2]. Untreated and continued injury leads to increased fibrosis, and when regenerative capacity fails, fibrotic response overwhelms parenchymal regeneration, leading to cirrhosis and its associated complications. Liver fibrosis is the single most important factor that determines the outcome in chronic liver disease (CLD). Early treatment of liver fibrosis is associated with better

✉Sudhakar K. Venkatesh, venkatesh.sudhakar@mayo.edu.

Conflict of interest All authors declare no conflict of interest to declare for this work.

outcomes, emphasizing the importance of early detection and assessment of severity of liver fibrosis [3–5]. The diagnosis of liver fibrosis can be established directly with histological evaluation from an invasive liver biopsy or indirectly by measuring surrogate markers for liver fibrosis. Although liver biopsy is considered the reference standard, it is associated with non-negligible complications, such as pain and bleeding, and it is limited by sampling error and low intra- and interobserver agreement [6]. Furthermore, the associated cost for liver biopsy makes it a less preferred method for follow up and response assessment, following treatment in CLD.

Non-invasive tests measure surrogate markers for the presence of liver fibrosis. The standard laboratory tests measure markers of liver inflammation and liver function that indirectly correlate to presence and severity of CLD. The direct biomarkers of fibrosis are not specific to liver fibrosis and can be influenced by fibrotic processes elsewhere in the body. The serum levels of these biomarkers also depend on their clearance from the body, which can be affected by other organ dysfunction [7]. A combination of direct and indirect biomarkers are used clinically in the form of indices such as AST-to-platelet ratio index (APRI) and FIB-4 score which are most useful for distinguishing cirrhosis from early stage fibrosis, but are not useful for differentiation of early stages of fibrosis.

The currently available imaging biomarkers for evaluation of liver fibrosis include: liver stiffness with ultrasound and MR elastography (MRE), restricted diffusion with diffusion weighted imaging (DWI), intra-voxel incoherent motion (IVIM) imaging, T1-relaxation on MRI, extracellular space estimation with CT or MRI, relative liver function estimation with gadoxetate-enhanced MRI, surface nodularity index on CT or MRI and attenuation differences with dual energy CT. Artificial intelligence and deep learning methods, including texture analysis, are also being explored with encouraging results. Of these, currently, liver stiffness evaluation (see Table 1 for description of terms used in the evaluation of mechanical properties of tissues) with ultrasound and MRE are validated in several studies and widely used in clinical practice Magnetic resonance elastography (MRE) measures stiffness of the liver by analyzing the propagation of shear waves through the liver [8]. MRE is currently regarded as the most accurate non-invasive diagnostic tool for detection and staging of liver fibrosis [9]. Although ultrasound-based elastography techniques have the added advantage of lower cost to the patient and accessibility, they are have lower accuracy, higher failure rate and lower reliability compared to MRE [10–12] rate. There is a continued debate as to which method is best, and the clinical use is usually determined by the availability of the method and local expertise at an institution.

Liver parenchymal stiffness is dependent on tissue composition, organization of the components, vascular component and interstitial pressure, and the pathological conditions affecting these factors [13]. In patients with CLD, destruction of normal hepatic parenchyma, progressive accumulation, and decreased remodeling of excessive extracellular matrix (ECM) and distortion of the parenchymal architecture lead to increased liver stiffness. Although liver fibrosis is the predominant factor that causes increased stiffness in CLD, other pathologic processes often coexisting with fibrosis, such as inflammation, biliary obstruction and cholestasis, passive congestion, and increased portal venous pressure may also contribute to increased liver stiffness [14, 15]. Differentiating these processes from liver

fibrosis is challenging and research work and efforts are being made in this direction with evaluation of other mechanical parameters obtained with MRE.

In this review article, we will briefly describe the current status of MRE of the liver in the evaluation of CLD and in the following section we will focus on future perspectives.

Current liver MRE technique

Liver MRE can be easily integrated into the existing clinical MR scanners. The widely available FDA-approved MRE pulse sequence is a phase contrast two-dimensional gradient recalled echo (2D GRE MRE) sequence. The clinical liver MRE setup includes an active pneumatic mechanical driver stationed outside the MRI scanning room and connected to a passive driver with a 25–30-foot-long flexible plastic tube. The passive driver is placed on the lower chest wall and right upper abdomen of the subject, overlying the liver, and securely held in contact with a fibroelastic band. The active driver produces continuous acoustic vibrations at 60 Hz that are transmitted to the passive driver via the tube. The passive driver then transmits the waves to the entire abdomen, including the liver. These acoustic waves produce microscopic shear displacement of tissues, which when imaged continuously by the motion sensitive MRE sequence synchronized to the mechanical waves, produces images of propagating shear waves also known as wave images. Typically, 4 slices of 5–10 mm thickness through the largest cross-section of the liver are obtained, avoiding the dome of the liver and the inferior portion of the liver, as slices through these regions of liver can result in high liver stiffness measurement (LSM). A magnitude image delineating the anatomy of the upper abdomen and a phase contrast image that shows propagating shear waves at the same level are immediately reconstructed and available at the scanner for review. An inversion algorithm installed in the scanner automatically processes the information in the magnitude and phase images and produces gray scale and colored stiffness maps. The stiffness maps are also known as elastograms. Where available, a confidence map is overlayed on these images to exclude regions in the liver and abdomen which are noisy and have less reliable stiffness data. A reader can then draw region of interest (ROI) within the confidence map over the liver, avoiding liver edge, artifacts, fissures, fossa, and regions of wave interference, to obtain a reliable LSM. Depending on the vendor specifications, the LSM measurements can be made either on the gray-scale images or the colored stiffness maps. The mechanical property measured with MRE is the magnitude of the complex shear modulus expressed in kilopascals (kPa). This mechanical property represents both elasticity and viscosity of the tissue. A mean LSM value from the ROIs drawn on the 4 obtained slices is reported for clinical purposes.

Liver stiffness measurement (LSM)

LSM measurement should ideally be performed with large regions of interest (ROI), drawn with free hand or automatically, covering as much as possible of the right lobe of the liver within the confidence map [16]. The left lobe is generally avoided due to pulsation artifacts from the overlying heart. The preferred method is a free hand geographical ROI that includes as large a liver parenchyma possible avoiding artifacts (Fig. 1). As liver fibrosis progresses in CLD, regions of the liver may have different degrees of fibrosis. This

heterogeneity of disease process is well known in most CLD and therefore smaller ROIs which do not adequately cover the entire available area for measurement may lead to inaccurate LSM (Fig. 2) [17].

MRE is highly reproducible with excellent to near perfect intra- and inter-observer agreement [18–21]. One reason the technique is highly reproducible is the ability of MRE to obtain LSM from a large portion of liver parenchyma. MRE of the liver is not significantly affected by the fatty change (hepatic steatosis) in the liver and can be easily performed even in obese individuals, as long as they are able to fit into the MR scanner [22–24]. Studies have shown that MRE is reproducible on different scanner platforms [25–27]. LSM with MRE is a physical property of the tissue and is not affected by the strength of the magnet. Similarly, studies have shown that LSM is not affected by the gadolinium-based contrast agents used for liver imaging [28].

The LSM obtained with MRE is dependent on the frequency of the applied mechanical waves and not comparable to LSM obtained at different frequencies either on MR or ultrasound. Furthermore, the inversion algorithms and assumptions for mechanical properties are different from ultrasound-based elastography. For example, the vibration controlled transient elastography (VCTE) method uses 50 Hz and measures Young's modulus which is about 3 times the shear modulus measured with MRE. Similarly, shear wave elastography measures at a wide frequency range (200–300 Hz) are not comparable with LSM obtained with MRE.

Limitations of current liver MRE technique

The 2D GRE-MRE technique is a gradient echo-based technique and is susceptible to the presence of paramagnetic substances that reduce parenchyma signal. The LSM is not affected by field strength of the magnet; however, a higher technical failure rate has been reported with 3T scanners (10.7% vs. 4.2%) [29] Technical failure accounts for less than 5% of examinations, with liver iron overload being the most common cause [30]. Other causes for technical failure include massive ascites, high body index with increased subcutaneous fat thickness, and poor contact between the passive driver and the anterior abdominal wall, all of which may result in poor transmission of shear waves into the liver. Failure of synchronization between active driver and MRE sequence can also result in suboptimal or failed MRE. Another cause for technical failure would be inconsistent breath holding by patients. Motion during the sequence can produce chaotic waves due to motion superimposed on shear waves and lead to inaccurate LSM.

The LSM obtained with standard clinical MRE sequence represents the stiffness of liver parenchyma and cannot differentiate between those caused by inflammation, congestion or increased vascular pressure. Therefore, the stiffness values should be interpreted carefully with clinical findings and laboratory tests as they would provide important clues for interpreting increased stiffness.

Current clinical applications of liver MRE in CLD

Detection and staging of liver fibrosis

Liver fibrosis results in increased stiffness in CLD as compared to normal livers. LSM with MRE can differentiate normal liver from fibrotic livers with > 90% accuracy [18, 22, 31, 32], and MRE can also detect early stages of fibrosis when cirrhotic morphology may not be present [33, 34]. The LSM increases as the stage of fibrosis progresses. The increase in liver stiffness occurs in small increments during early stages of fibrosis (stages 0 through 2), but in larger increments and almost exponentially in advanced stages of fibrosis (stages 3 and 4). This biphasic increase in liver stiffness correlates with the proportion of fibrotic tissue in liver parenchyma during early and later stages of fibrosis [35–37]. The smaller incremental difference in stiffness during early stages also poses a challenge to accurate differentiation between the early stages (stage 0–2). Larger differences in liver stiffness exists between advanced fibrosis/cirrhosis and early stage fibrosis and is, therefore, easier to differentiate with MRE and other elastography techniques.

The utility of MRE in detection of fibrosis in major causes of CLD, such as chronic hepatitis B (CHB), chronic hepatitis C (CHC), alcoholic liver disease (ALD), and nonalcoholic fatty liver disease (NAFLD), has been demonstrated in multiple studies [31, 32, 38–50]. Meta-analysis studies with pooled data from multiple institutions have confirmed higher performance of MRE [23, 30]. The usefulness of MRE in detection of liver fibrosis in uncommon chronic liver diseases, such as primary sclerosing cholangitis (PSC) and for detection of advanced fibrosis in autoimmune hepatitis, has also been demonstrated [51–56]. The pathological changes are heterogeneous and unique; different processes occur in different etiologies. For example, macronodular cirrhosis is common in chronic hepatitis B whereas micro-nodular cirrhosis occurs more frequently in chronic hepatitis C; ballooning of hepatocytes occurs in NASH; chronic lymphocytic infiltrate is common in autoimmune hepatitis and primary biliary cirrhosis; and periductal fibrosis in primary sclerosing cholangitis. It is, therefore, expected that the LSM cutoffs to differentiate fibrotic stages would not be similar for different etiologies (Table 2). Reported studies have been heterogeneous in terms of patient selection and histologic methods of staging fibrosis (Ishak score vs. METAVIR score, etc.,) and, therefore, direct comparison of LSM cutoffs for different etiologies has been lacking [57]. With the widespread use of non-invasive tests for diagnosis of fibrosis, the likelihood a comparison study of such nature would also be challenging to perform in the future. In routine clinical practice at our institute we find it easy and practical to use a simplified classification of liver fibrosis using MRE LSM (Table 3). The cut-offs were derived using large database of patients undergoing MRE and pathological correlation wherever possible and from a clinical management perspective. It would be most useful to rule in fibrosis to assist initiation of treatment and rule out cirrhosis for determining the need for surveillance of complications-portal hypertension, bleeding esophageal varices and hepatocellular carcinoma.

MRE is established as a robust, reliable, and accurate non-invasive test for evaluation of liver fibrosis. Several studies have also shown superior performance of MRE compared to serum liver tests [58]. Many studies have also shown similar or superior performance of MRE

compared to VCTE and shear wave elastography (SWE). A number of studies have also shown better performance of MRE compared with DWI, IVIM, surface nodularity, T1-mapping, T2-mapping, liver and spleen volumetry, extracellular space fraction estimation and relative liver enhancement ratio with gadoxetate [59–64].

Currently, there are different cutoffs proposed for distinguishing fibrosis stages in different CLDs (Table 2). The rationale for distinguishing stages of fibrosis for clinical use arose from the need for management decisions in CLD. Previously, clinically significant fibrosis stage (stage 2 or higher) was considered optimal for treatment of fibrosis, and in patients with advanced fibrosis (stage 3 or higher) were considered suitable for surveillance of complications. However, these goals continue to evolve as treatment options become available. A simple and practical classification of LSM would be useful for general practice (Table 3) as discussed above [65]. The interpretation of the LSM should always be made in reference to clinical context and to available liver function tests results.

Follow–up assessment

As fibrosis is the major determinant of outcome in CLD, assessment of progression in patients on follow up is important (Fig. 3). MRE is well suited for longitudinal follow up of patients with CLD [66]. A 20% change in mean LSM under identical conditions is a significant change in the LSM in the longitudinal assessment [21]. Takamura et al., showed that MRE is useful in stratifying the risk of clinical progression of cirrhosis from Child–Pugh class A to B in chronic hepatitis C patients [44]. Higher LSM is associated with development of complications including HCC, portal hypertension and decompensation as discussed below.

Association of liver stiffness and hepatocellular carcinoma

Patients with CLD are at high risk of development hepatocellular carcinoma (HCC). LSM with MRE is an independent risk factor for development of HCC in patients with CLD [67]. In one study, patients with LSM > 4.44 kPa had a higher incidence of HCC occurrence (36.4% vs. 9.5%) than patients with LSM < 4.44 kPa [68]. Yasui et al. showed that LSM > 4.6 kPa was an independent factor associated with HCC development in chronic hepatitis C patients [69]. In an another study, Ichikawa et al. showed that patients with LSM > 4.7 kPa were at high risk of developing a HCC [70]. Tamaki et al. in a study of patients with HCC with sustained virological response, showed that an LSM cutoff ≥ 3.75 kPa was predictive of HCC development. In patients with HCC and undergoing treatment, a LSM > 5.5 kPa is also predictive of early recurrence of HCC following treatment, suggesting careful follow up in patients with high pretreatment LSM [71]. In addition, a high tumor stiffness of HCC may also be useful for prediction of recurrence [72].

Portal hypertension

Patients with advanced fibrosis are at risk of developing portal hypertension. Bleeding esophageal varices is the most significant manifestation of portal hypertension and carries a very high mortality rate. Several studies have shown the feasibility and utility of MRE in prediction of esophageal varices, either with LSM or spleen stiffness measurements [73, 74]. Both LSM and spleen stiffness have been shown to have high accuracy in predicting

esophageal varices [75–77], and spleen stiffness has been shown to be more predictive of severe, high risk or clinically significant esophageal varices [74, 78]. For practical purposes, a high LSM, particularly > 5 kPa, is associated with increased risk of portal hypertension and esophageal varices.

Prediction of decompensation

Decompensation in patients with advanced liver fibrosis can also be predicted with MRE. Asrani et al. demonstrated in a population of chronic hepatitis C patients that a baseline LSM ≥ 5.8 kPa had a higher risk of decompensation (Hazards ratio 4.96) [79]. Similarly, Eaton et al. showed that LSM ≥ 6 kPa had a high risk for hepatic decompensation in patients with primary sclerosing cholangitis [52] Lee et al., in a 217 patient population with multiple etiologies for CLD but predominantly (75%) hepatitis B or C, showed that LSM was significantly associated with decompensation and overall survival [68]. Further, it has been shown that a single LSM with MRE and changes in LSM over time are independently associated with hepatic decompensation in patients with PSC [53]. Baseline LSM can, therefore, be used for close monitoring of patients with advanced fibrosis who are at higher risk of decompensation.

Nonalcoholic fatty liver disease (NAFLD)

NAFLD is the most common cause of CLD with increasing prevalence [80]. NAFLD is a spectrum of disease with nonalcoholic fatty liver (NAFL) which carries no increased risk of mortality at one end to nonalcoholic steatohepatitis (NASH) with increased risk of mortality due to both liver-related and cardiovascular events at the other end of the spectrum [81, 82]. Distinction between NAFL and NASH would be of paramount importance for risk stratification (Fig. 4). Similar to other CLD, liver fibrosis is also the single most important feature that predicts outcome in NAFLD. Preliminary studies showed high sensitivity and specificity for distinguishing NAFL from NASH, and NAFL from advanced fibrosis [46, 47]. In a prospective study, Loomba et al. suggested that a cutoff value of 3.26 kPa for discriminating NASH from NAFL which was similar to another study by Costa-Silva et al., who reported a cutoff of 3.2 kPa [48, 49]

In a meta-analysis including 9 studies and 232 patients with NAFLD, LSM cutoffs of 2.88, 3.54, 3.77 and 4.09 kPa discriminated fibrosis stages 1, 2, 3 and cirrhosis, respectively [23]. In a recent meta-analysis, the accuracy of MRE was 0.96 for diagnosis of advanced fibrosis and 0.92 for diagnosis of cirrhosis with cutoff values of 3.62–4.8 kPa and 4.15–6.7 kPa, respectively [10]. In a study comparing 2D-MRE and clinical prediction rules for NAFLD for diagnosing advanced fibrosis, it was shown that 2D-MRE had significantly better AUROC versus clinical prediction rules [83]. Research in utility of MRE in NAFLD will continue as the prevalence of the disease increases and as newer methods of treatment may emerge. Currently, the main utility of MRE in NAFLD is distinguishing NAFL from NASH and in stratification of patients with advanced fibrosis from those with mild or no fibrosis for management purposes.

MRE in the pediatric population

MRE has been successfully utilized in the evaluation of CLD in chronic liver disease and its application in the pediatric population and is expanding [84–86]. MRE technique is reportedly successful in pediatric and young adults [87]. While normal liver stiffness values are shown to be lower in pediatric subjects compared to adults, a recent study with children showed that liver stiffness was higher than expected, suggesting clarification in future studies [88, 89].

MRE in liver transplants

Liver transplants are at risk of recurrence of CLD, such as viral hepatitis, autoimmune liver diseases and NAFLD. MRE can be performed on the liver grafts (Fig. 5), however, it should be avoided in the immediate post-transplantation period [90]. The immediate post-transplantation period may be accompanied by edema, congestion and inflammation, which can result in increased liver stiffness. MRE is very useful for detection of recurrence of fibrosis in the graft [91–93]. MRE can also be used in the evaluation of potential donors for detection of occult fibrosis [90].

Advances in liver MRE

Hardware

A consistent and good contact between the passive driver and the patient is necessary for better transmission of acoustic vibrations to obtain high-quality elastograms. To further improve the patient experience during the scan, a rectangular flexible and soft pneumatic driver has been developed recently (Fig. 6) [94]. Compared to the conventional round rigid driver, the flexible and soft driver can cover more of the liver, which enables the propagation of more uniform shear waves and, potentially, improves the liver stiffness estimation accuracy [66]. A recent study showed similar LSM obtained with the new driver compared to a conventional driver in a normal healthy volunteer population [95]. A smaller, rectangular driver made of similar material can be used in the pediatric population. An implementation of multiple acoustic drivers can further improve accessibility of MRE assessment for many other abdominal organs, such as spleen and kidney, which could be affected in the development of chronic liver diseases.

MRE sequence

Several advances have been made in the MRE sequence to improve technical success and to address limitations. First, the duration of breath hold for MRE has been significantly shortened to about 11–12 s for each slice which improves patient comfort as well. The conventional MRE should be performed under breath holds at the end of expiration, to avoid respiratory motion artifacts [17, 18]. The acquisition time can also be reduced with the use of parallel imaging and reduced k-space acquisition [96]. However, pediatric and sedated patients may have difficulty performing adequate breath holds. A free-breathing MRE would be useful in patients who have difficulty holding breath due to comorbidities. Studies have shown similar results with free-breathing MRE, respiratory-navigated and conventional breath hold MRE [96, 97]. A non-gated, free-breathing, single-shot, multi-slice 2D EPI-

MRE technique with a view-sharing-based reconstruction strategy [98], has been developed. This free-breathing MRE can provide accurate liver stiffness measurements and comparable repeatability, compared with conventional breath-held MRE [99]. Additionally, this non-gate free-breathing MRE enables liver stiffness to be measured over respiratory cycles, which may provide another mechanical parameter reflecting states of disease progression [100].

Spin-echo Echo-planar imaging MRE (SE-EPIMRE) with a rapid readout allows faster acquisition, which can be utilized to obtain multiple sections in one breath hold. The time to echo (TE) of the SE-EPI MRE is typically shorter than the conventional 2D GREMRE sequence, which helps in higher liver parenchymal signal and results in better elastograms. Several studies have shown excellent results with SE-EPIMRE, both in adults and in children and young adults [84, 101], with many studies showing significant advantages of SE-EPIMRE over 2D-GREMRE technique, particularly, higher technical success [42, 102]. A pooled meta-analysis showed equivalent performance of SE-EPIMRE and 2D-GREMRE for detection and staging of liver fibrosis [103].

SE-EPI MRE is also useful in patients with mild iron overload of the liver due to its shorter TE (Fig. 7). However, if the iron overload is severe, even SE-EPI MRE can also fail. In such rare situations, alternative methods of assessment for liver fibrosis may be employed or MRE can be attempted once liver iron overload is treated.

3D MRE

The conventional 2D MRE sequence is sensitized to detect motion in one plane (i.e., perpendicular to the axial plane) and works on the principle that shear waves are propagating through the axial plane of acquisition. However, this assumption is not always true, particularly in the regions of liver near the dome and inferiorly or further away from the passive driver. The waves in these regions may be propagating oblique to the axial plane that may lead to overestimation of the wavelength of shear waves. A three-dimensional MRE sequence (3D MRE) sensitized to detect motion in all three planes can correct for obliquity of waves. 3D MRE sequence is usually spin echo (SE)-based and allows for a large volume of liver to be evaluated with a few breathholds. The number of slices typically ranges from 32 to 40. As the 3D MRE sequence corrects for obliquity of the waves, the LSM obtained may be slightly lower than those obtained with conventional sequence [104]. Studies have shown a better diagnostic performance of 3D MRE and lower failure rate [50].

Multi−parametric MRE

Some investigations demonstrated the feasibility of multi-parametric MRE, which provides multiple mechanical properties that may be sensitive to different pathophysiologic processes [105–114]. Besides well-accepted shear stiffness that is associated with fibrosis, the dispersions of shear wave velocity and attenuation were found to be associated with the degree of steatosis [115]. Yin et al. found the damping ratio and the loss modulus increase significantly at the early onset of liver injury or necroinflammation [116]. The slip interface imaging that provides information about boundary conditions of the focal lesions may be used to predict interface adhesiveness and invasiveness of liver tumor [117].

In one study of NAFLD cohort undergoing bariatric surgery, Allen et al. demonstrated that parameters obtained with multifrequency 3D MRE can provide imaging biomarkers for NASH diagnosis and monitoring. Combining fat fraction obtained with proton density fat fraction (PDFF) estimation with damping ratio at 40 Hz and shear stiffness at 60 Hz correlated best with NASH activity and could predict early NASH activity [118]. They used a predictive model using shear stiffness, damping ratio and MRI-PDFF (Fig. 8). In a follow-up study, the same investigators showed that multi-parametric MRE improves detection of NASH regression following bariatric surgery [119].

Incorporating augmented human intelligence and deep learning

Advantages of MRE over other elastographic techniques include the ability to evaluate the entire liver parenchyma, and standardization across manufacturer platforms (GE, Siemens, and Philips) and field strength (1.5T and 3.0T), since the vast majority of MRE hardware and software currently comes from a single company (Resoundant, Inc., Rochester, MN)To minimize the inter-observer variation and release radiologists from manual analysis, a fully automated segmentation algorithm, automated liver elasticity calculation (ALEC), has been developed for liver stiffness measurement (Fig. 9). ALEC has been demonstrated to be highly consistent with the manual measurements in both 2D MRE and 3D MRE [120, 121]. Although ALEC is currently used in only one major institution, it is expected to be available for use at other institutes, soon.

Neural network inversion may be applied to inversion algorithms that convert the shear wave data into stiffness maps for improving accuracy and resolution [122]. This work is promising for accurate characterization of focal liver lesions.

Emerging applications of liver MRE

Several pathological processes can increase liver stiffness and therefore confound the detection of liver fibrosis in CLD. These include passive vascular congestion, inflammation and portal hypertension. The current standard MRE may not be able to differentiate these processes, but still provides valuable information on the effect on liver stiffness.

Congestive hepatopathy

Passive venous congestion due to increased central venous pressure leads to congestive hepatopathy. Congestive hepatopathy can result from different etiologies including congestive cardiac failure from any cause, congenital cardiac anomalies, tricuspid regurgitation, constrictive pericarditis, and hepatic venous obstruction including Budd-Chiari syndrome. Chronic congestion finally leads to cirrhosis if severe and long standing. The congestion causes increase in liver stiffness and result in abnormally elevated LSM, and the increase in LSM is also related to the duration of the disease. Due attention needs to be paid to the presence of congestion and avoid false interpretation of elevated LSM as liver fibrosis. In these situations, a comprehensive MRI + MRE provides valuable clues for the presence of other causes (congestion, inflammation, biliary obstruction) and should be interpreted by considering the clinical information and liver function test results. Patients with congenital single ventricle disease have been treated successfully with Fontan surgery. However post-

Fontan, these patients develop venous congestion termed as Fontan-associated liver disease (FALD). FALD leads to increased liver stiffness that can be detected by MRE (Fig. 10) and the increased liver stiffness is related to duration of FALD [86, 123]. An inverse relationship exists between LSM and cardiac index [86, 124]. In one study, Poterucha et al. showed that mean LSM was higher in patients with malignant nodules compared to those with benign nodules [124, 125]. Liver stiffness was independently associated with central venous pressure [126] and a LSM > 4 kPa was associated with central venous pressure > 14 mmHg [127]. LSM also correlates with MELD score in FALD and congestive hepatic fibrosis score [127, 128]. A LSM > 5 kPa is associated with bridging fibrosis and cirrhosis [127]. MRE is also useful in follow up of FALD. Increased LSM may serve as a global imaging biomarker of FALD and an annual increase in LS of > 0.3 kPa was associated with increased morbidity [128, 129].

Diffuse infiltrative disorders

Infiltrative disorders can lead to increased liver stiffness secondary to the effect of deposition (e.g., amyloidosis) or associated fibrotic changes (e.g., Gaucher's disease). MRE may be clinically indicated in these patients for suspected liver fibrosis due to abnormal liver function tests. The increased LSM should be carefully interpreted as the stiffness need not represent fibrosis. In amyloidosis, deposition of amyloid fibrils in the perisinusoidal space may increase liver stiffness and a correlation between LSM and degree of liver dysfunction has been reported [130]. Storage disorders like Gaucher's may result in liver fibrosis and MRE may be useful in monitoring the progress of liver fibrosis [131]. A recent study by Serai et al. showed that LSM correlates with disease severity scoring system in Gaucher disease type 1 patients [132]. More studies are required to establish the role of MRE in evaluation of these disorders. In clinical practice, abnormally high LSM in an otherwise morphologically normal liver or enlarged liver with no CLD and cardiac disease should raise suspicion for infiltrative etiology.

Differentiate non-cirrhotic portal hypertension from cirrhotic portal hypertension

Non-cirrhotic portal hypertension (NCPH) can result from extrahepatic causes including portal vein and splenic vein thrombosis or a hepatic cause, like nodular regenerative hyperplasia (NRH). Clinically differentiating NCPH from cirrhotic portal hypertension (CPH) can be difficult, especially when patients present late in the course of the disease. Often, the liver is dysmorphic due to redistributed portal flow leading to regions of hypertrophy and atrophy simulating cirrhosis. However, in the early stages, the liver morphology is usually normal and liver stiffness is not significantly elevated (Fig. 11). MRE demonstrates significantly lower LSM in these patients as compared to CPH [133, 134], however, the liver stiffness may still be above normal [135]. Measuring spleen stiffness and computing spleen stiffness to liver stiffness ratio may also be helpful [133, 134]. Absence of risk factor for chronic liver disease, preserved liver function and mild to moderately elevated LSM (< 5 kPa) is useful information to suspect NCPH.

MRE in clinical trials for treatment response

MRE may provide the much-needed non-invasive alternative for assessment of treatment response in clinical trials. Several trials in NAFLD have used MRE-derived liver stiffness combined with PDFF as surrogate end points [136–139].

Other applications

MRE-derived LSM represents fibrosis burden and can be used as a surrogate for liver function. Baseline LSM has been shown to predict functional hepatic failure following partial hepatectomy and stereotactic body radiation therapy [140, 141]. This pretreatment information may be useful in planning treatment methods and close follow up of patients who will be at higher risk of decompensation

Summary and conclusions

Liver MRE is currently considered the most accurate non-invasive technique for detection and staging of liver fibrosis. The utility of MRE in chronic liver disease from various etiologies has been established. Improvements in technique have made MRE faster and more comfortable for patients with increasing applications in the pediatric population. Multiple parameters from advanced MRE sequences provide for characterization of different chronic liver diseases, and an opportunity for earlier detection of disease and in the follow-up assessment. Newer clinical applications continue to emerge in this dynamic and exciting field of elastography Table 4.

Acknowledgements

The authors acknowledge the assistance of Lucy Bahn, PhD, in preparation of this manuscript. Dr. Meng Yin acknowledges the support from NIH grant (EB017197) and U.S. Department of Defense grant (W81XWH-19-1-0583-01). Dr. Sudhakar Venkatesh acknowledges support from U.S. Department of Defense grant (W81XWH-19-1-0583-01) and NIH grant R37 EB001981.

Funding No funding received for this work.

References

1. Byass P The global burden of liver disease: a challenge for methods and for public health. BMC Med 2014; 12:159 [PubMed: 25286285]
2. Parola M, Pinzani M. Liver fibrosis: Pathophysiology, pathogenetic targets and clinical issues. Mol Aspects Med 2019; 65:37–55 [PubMed: 30213667]
3. Martinez SM, Foucher J, Combis JM, et al. Longitudinal liver stiffness assessment in patients with chronic hepatitis C undergoing antiviral therapy. PLoS One 2012; 7:e47715 [PubMed: 23082200]
4. Marcellin P, Gane E, Buti M, et al. Regression of cirrhosis during treatment with tenofovir disoproxil fumarate for chronic hepatitis B: a 5-year open-label follow-up study. Lancet 2013; 381:468–475 [PubMed: 23234725]
5. Campana L, Iredale JP. Regression of Liver Fibrosis. Semin Liver Dis 2017; 37:1–10 [PubMed: 28201843]
6. Regev A, Berho M, Jeffers LJ, et al. Sampling error and intraobserver variation in liver biopsy in patients with chronic HCV infection. The American journal of gastroenterology 2002; 97:2614–2618 [PubMed: 12385448]
7. Baranova A, Lal P, Birerdinc A, Younossi ZM. Non-invasive markers for hepatic fibrosis. BMC Gastroenterol 2011; 11:91 [PubMed: 21849046]

8. Venkatesh SK, Yin M, Ehman RL. Magnetic resonance elastography of liver: technique, analysis, and clinical applications. J Magn Reson Imaging 2013; 37:544–555 [PubMed: 23423795]
9. Bashir M, Horowitz J, Kamel I, et al. ACR Appropriateness Criteria Chronic Liver Disease. Available at https://acsearch.acr.org/docs/3098416/Narrative/. American College of Radiology.
10. Xiao G, Zhu S, Xiao X, Yan L, Yang J, Wu G. Comparison of laboratory tests, ultrasound, or magnetic resonance elastography to detect fibrosis in patients with nonalcoholic fatty liver disease: A meta-analysis. Hepatology 2017; 66:1486–1501 [PubMed: 28586172]
11. Yoon JH, Lee JM, Woo HS, et al. Staging of hepatic fibrosis: comparison of magnetic resonance elastography and shear wave elastography in the same individuals. Korean J Radiol 2013; 14:202–212 [PubMed: 23483022]
12. Huwart L, Sempoux C, Vicaut E, et al. Magnetic resonance elastography for the noninvasive staging of liver fibrosis. Gastroenterology 2008; 135:32–40 [PubMed: 18471441]
13. Mueller S, Sandrin L. Liver stiffness: a novel parameter for the diagnosis of liver disease. Hepat Med 2010; 2:49–67 [PubMed: 24367208]
14. Venkatesh SK, Wells ML, Miller FH, et al. Magnetic resonance elastography: beyond liver fibrosis-a case-based pictorial review. Abdom Radiol (NY) 2018; 43:1590–1611 [PubMed: 29143076]
15. Ichikawa S, Motosugi U, Nakazawa T, et al. Hepatitis activity should be considered a confounder of liver stiffness measured with MR elastography. J Magn Reson Imaging 2015; 41:1203–1208 [PubMed: 24889753]
16. Guglielmo FF, Venkatesh SK, Mitchell DG. Liver MR Elastography Technique and Image Interpretation: Pearls and Pitfalls. Radiographics 2019; 39:1983–2002 [PubMed: 31626569]
17. Rezvani Habibabadi R, Khoshpouri P, Ghadimi M, et al. Comparison between ROI-based and volumetric measurements in quantifying heterogeneity of liver stiffness using MR elastography. Eur Radiol 2020; 30:1609–1615 [PubMed: 31705257]
18. Venkatesh SK, Wang G, Teo LL, Ang BW. Magnetic resonance elastography of liver in healthy Asians: normal liver stiffness quantification and reproducibility assessment. J Magn Reson Imaging 2014; 39:1–8 [PubMed: 24123300]
19. Shire NJ, Yin M, Chen J, et al. Test-retest repeatability of MR elastography for noninvasive liver fibrosis assessment in hepatitis C. J Magn Reson Imaging 2011; 34:947–955 [PubMed: 21751289]
20. Lee Y, Lee JM, Lee JE, et al. MR elastography for noninvasive assessment of hepatic fibrosis: reproducibility of the examination and reproducibility and repeatability of the liver stiffness value measurement. J Magn Reson Imaging 2014; 39:326–331 [PubMed: 23589232]
21. Serai SD, Obuchowski NA, Venkatesh SK, et al. Repeatability of MR Elastography of Liver: A Meta-Analysis. Radiology 2017; 285:92–100 [PubMed: 28530847]
22. Yin M, Talwalkar JA, Glaser KJ, et al. Assessment of hepatic fibrosis with magnetic resonance elastography. Clinical gastroenterology and hepatology : the official clinical practice journal of the American Gastroenterological Association 2007; 5:1207–1213.e1202 [PubMed: 17916548]
23. Singh S, Venkatesh SK, Loomba R, et al. Magnetic resonance elastography for staging liver fibrosis in non-alcoholic fatty liver disease: a diagnostic accuracy systematic review and individual participant data pooled analysis. Eur Radiol 2016; 26:1431–1440 [PubMed: 26314479]
24. Cui J, Heba E, Hernandez C, et al. Magnetic resonance elastography is superior to acoustic radiation force impulse for the Diagnosis of fibrosis in patients with biopsy-proven nonalcoholic fatty liver disease: A prospective study. Hepatology (Baltimore, Md) 2016; 63:453–461
25. Serai SD, Yin M, Wang H, Ehman RL, Podberesky DJ. Cross-vendor validation of liver magnetic resonance elastography. Abdom Imaging 2015; 40:789–794 [PubMed: 25476489]
26. Trout AT, Serai S, Mahley AD, et al. Liver Stiffness Measurements with MR Elastography: Agreement and Repeatability across Imaging Systems, Field Strengths, and Pulse Sequences. Radiology 2016; 281:793–804 [PubMed: 27285061]
27. Yasar TK, Wagner M, Bane O, et al. Interplatform reproducibility of liver and spleen stiffness measured with MR elastography. J Magn Reson Imaging 2016; 43:1064–1072 [PubMed: 26469708]
28. Hallinan JT, Alsaif HS, Wee A, Venkatesh SK. Magnetic resonance elastography of liver: influence of intravenous gadolinium administration on measured liver stiffness. Abdom Imaging 2015; 40:783–788 [PubMed: 25331568]

29. Kim DW, Kim SY, Yoon HM, Kim KW, Byun JH. Comparison of technical failure of MR elastography for measuring liver stiffness between gradient-recalled echo and spin-echo echo-planar imaging: A systematic review and meta-analysis. J Magn Reson Imaging 2020; 51:1086–1102 [PubMed: 31456328]
30. Singh S, Venkatesh SK, Wang Z, et al. Diagnostic performance of magnetic resonance elastography in staging liver fibrosis: a systematic review and meta-analysis of individual participant data. Clinical gastroenterology and hepatology : the official clinical practice journal of the American Gastroenterological Association 2015; 13:440–451.e446 [PubMed: 25305349]
31. Venkatesh SK, Wang G, Lim SG, Wee A. Magnetic resonance elastography for the detection and staging of liver fibrosis in chronic hepatitis B. Eur Radiol 2014; 24:70–78 [PubMed: 23928932]
32. Ichikawa S, Motosugi U, Ichikawa T, et al. Magnetic resonance elastography for staging liver fibrosis in chronic hepatitis C. Magn Reson Med Sci 2012; 11:291–297 [PubMed: 23269016]
33. Venkatesh SK, Yin M, Takahashi N, Glockner JF, Talwalkar JA, Ehman RL. Non-invasive detection of liver fibrosis: MR imaging features vs. MR elastography. Abdominal imaging 2015; 40:766–775 [PubMed: 25805619]
34. Rustogi R, Horowitz J, Harmath C, et al. Accuracy of MR Elastography and Anatomic MR Imaging Features in the Diagnosis of Severe Hepatic Fibrosis and Cirrhosis. Journal of magnetic resonance imaging : JMRI 2012; 35:1356–1364 [PubMed: 22246952]
35. Venkatesh SK, Xu S, Tai D, Yu H, Wee A. Correlation of MR elastography with morphometric quantification of liver fibrosis (Fibro-C-Index) in chronic hepatitis B. Magn Reson Med 2014; 72:1123–1129 [PubMed: 24166665]
36. Standish RA, Cholongitas E, Dhillon A, Burroughs AK, Dhillon AP. An appraisal of the histopathological assessment of liver fibrosis. Gut 2006; 55:569–578 [PubMed: 16531536]
37. Masugi Y, Abe T, Tsujikawa H, et al. Quantitative assessment of liver fibrosis reveals a nonlinear association with fibrosis stage in nonalcoholic fatty liver disease. Hepatol Commun 2018; 2:58–68 [PubMed: 29404513]
38. Bohte AE, de Niet A, Jansen L, et al. Non-invasive evaluation of liver fibrosis: a comparison of ultrasound-based transient elastography and MR elastography in patients with viral hepatitis B and C. European Radiology 2014; 24:638–648 [PubMed: 24158528]
39. Lee JE, Lee JM, Lee KB, et al. Noninvasive assessment of hepatic fibrosis in patients with chronic hepatitis B viral infection using magnetic resonance elastography. Korean J Radiol 2014; 15:210–217 [PubMed: 24643284]
40. Ichikawa S, Motosugi U, Morisaka H, et al. Validity and Reliability of Magnetic Resonance Elastography for Staging Hepatic Fibrosis in Patients with Chronic Hepatitis B. Magn 2015; 14:211–221
41. Wu WP, Chou CT, Chen RC, Lee CW, Lee KW, Wu HK. Non-Invasive Evaluation of Hepatic Fibrosis: The Diagnostic Performance of Magnetic Resonance Elastography in Patients with Viral Hepatitis B or C. PLoS ONE [Electronic Resource] 2015; 10:e0140068
42. Shi Y, Xia F, Li QJ, et al. Magnetic Resonance Elastography for the Evaluation of Liver Fibrosis in Chronic Hepatitis B and C by Using Both Gradient-Recalled Echo and Spin-Echo Echo Planar Imaging: A Prospective Study. The American journal of gastroenterology 2016; 111:823–833 [PubMed: 26977760]
43. Hennedige TP, Wang G, Leung FP, et al. Magnetic Resonance Elastography and Diffusion Weighted Imaging in the Evaluation of Hepatic Fibrosis in Chronic Hepatitis B. Gut Liver 2017; 11:401–408 [PubMed: 27965475]
44. Takamura T, Motosugi U, Ichikawa S, et al. Usefulness of MR elastography for detecting clinical progression of cirrhosis from child-pugh class A to B in patients with type C viral hepatitis. J Magn Reson Imaging 2016; 44:715–722 [PubMed: 26929192]
45. Bensamoun SF, Leclerc GE, Debernard L, et al. Cutoff values for alcoholic liver fibrosis using magnetic resonance elastography technique. Alcohol Clin Exp Res 2013; 37:811–817 [PubMed: 23216352]
46. Chen J, Talwalkar JA, Yin M, Glaser KJ, Sanderson SO, Ehman RL. Early Detection of Nonalcoholic Steatohepatitis in Patients with Nonalcoholic Fatty Liver Disease by Using MR Elastography. Radiology 2011; 259:749–756 [PubMed: 21460032]

47. Kim D, Kim WR, Talwalkar JA, Kim HJ, Ehman RL. Advanced fibrosis in nonalcoholic fatty liver disease: noninvasive assessment with MR elastography. Radiology 2013; 268:411–419 [PubMed: 23564711]
48. Loomba R, Wolfson T, Ang B, et al. Magnetic resonance elastography predicts advanced fibrosis in patients with nonalcoholic fatty liver disease: a prospective study. Hepatology (Baltimore, Md) 2014; 60:1920–1928
49. Costa-Silva L, Ferolla SM, Lima AS, Vidigal PVT, Ferrari TCA. MR elastography is effective for the non-invasive evaluation of fibrosis and necroinflammatory activity in patients with nonalcoholic fatty liver disease. Eur J Radiol 2018; 98:82–89 [PubMed: 29279175]
50. Loomba R, Cui J, Wolfson T, et al. Novel 3D Magnetic Resonance Elastography for the Noninvasive Diagnosis of Advanced Fibrosis in NAFLD: A Prospective Study. The American journal of gastroenterology 2016; 111:986–994 [PubMed: 27002798]
51. Bookwalter CA, Venkatesh SK, Eaton JE, Smyrk TD, Ehman RL. MR elastography in primary sclerosing cholangitis: correlating liver stiffness with bile duct strictures and parenchymal changes. Abdom Radiol (NY) 2018; 43:3260–3270 [PubMed: 29626258]
52. Eaton JE, Dzyubak B, Venkatesh SK, et al. Performance of magnetic resonance elastography in primary sclerosing cholangitis. J Gastroenterol Hepatol 2016; 31:1184–1190 [PubMed: 26691631]
53. Eaton JE, Sen A, Hoodeshenas S, et al. Changes in Liver Stiffness, Measured by Magnetic Resonance Elastography, Associated With Hepatic Decompensation in Patients With Primary Sclerosing Cholangitis. Clinical gastroenterology and hepatology : the official clinical practice journal of the American Gastroenterological Association 2019;
54. Idilman IS, Low HM, Bakhshi Z, Eaton J, Venkatesh SK. Comparison of liver stiffness measurement with MRE and liver and spleen volumetry for prediction of disease severity and hepatic decompensation in patients with primary sclerosing cholangitis. Abdom Radiol (NY) 2020; 45:701–709 [PubMed: 31894383]
55. Wang J, Malik N, Yin M, et al. Magnetic resonance elastography is accurate in detecting advanced fibrosis in autoimmune hepatitis. World J Gastroenterol 2017; 23:859–868 [PubMed: 28223730]
56. Jhaveri KS, Hosseini-Nik H, Sadoughi N, et al. The development and validation of magnetic resonance elastography for fibrosis staging in primary sclerosing cholangitis. Eur Radiol 2019; 29:1039–1047 [PubMed: 30051141]
57. Chang W, Lee JM, Yoon JH, et al. Liver Fibrosis Staging with MR Elastography: Comparison of Diagnostic Performance between Patients with Chronic Hepatitis B and Those with Other Etiologic Causes. Radiology 2016; 280:88–97 [PubMed: 26844364]
58. Xu XY, Wang WS, Zhang QM, et al. Performance of common imaging techniques. World J Clin Cases 2019; 7:2022–2037 [PubMed: 31423434]
59. Hennedige TP, Hallinan JT, Leung FP, et al. Comparison of magnetic resonance elastography and diffusion-weighted imaging for differentiating benign and malignant liver lesions. Eur Radiol 2016; 26:398–406 [PubMed: 26032879]
60. Fu F, Li X, Chen C, et al. Non-invasive assessment of hepatic fibrosis: comparison of MR elastography to transient elastography and intravoxel incoherent motion diffusion-weighted MRI. Abdom Radiol (NY) 2020; 45:73–82 [PubMed: 31372777]
61. Wang Y, Ganger DR, Levitsky J, et al. Assessment of chronic hepatitis and fibrosis: comparison of MR elastography and diffusion-weighted imaging. AJR Am J Roentgenol 2011; 196:553–561 [PubMed: 21343496]
62. Besa C, Wagner M, Lo G, et al. Detection of liver fibrosis using qualitative and quantitative MR elastography compared to liver surface nodularity measurement, gadoxetic acid uptake, and serum markers. J Magn Reson Imaging 2018; 47:1552–1561 [PubMed: 29193508]
63. Hoffman DH, Ayoola A, Nickel D, Han F, Chandarana H, Shanbhogue KP. T1 mapping, T2 mapping and MR elastography of the liver for detection and staging of liver fibrosis. Abdom Radiol (NY) 2020; 45:692–700 [PubMed: 31875241]
64. Kim JW, Lee YS, Park YS, et al. Multiparametric MR Index for the Diagnosis of Non-Alcoholic Steatohepatitis in Patients with Non-Alcoholic Fatty Liver Disease. Sci Rep 2020; 10:2671 [PubMed: 32060386]

65. Venkatesh SK, Ehman RL. Magnetic resonance elastography of liver. Magn Reson Imaging Clin N Am 2014; 22:433–446 [PubMed: 25086938]
66. Venkatesh SK, Wells ML, Miller FH, et al. Magnetic resonance elastography: beyond liver fibrosis-a case-based pictorial review. Abdom Radiol (NY) 2017
67. Motosugi U, Ichikawa T, Koshiishi T, et al. Liver stiffness measured by magnetic resonance elastography as a risk factor for hepatocellular carcinoma: a preliminary case-control study. Eur Radiol 2013; 23:156–162 [PubMed: 22814828]
68. Lee DH, Lee JM, Chang W, et al. Prognostic Role of Liver Stiffness Measurements Using Magnetic Resonance Elastography in Patients with Compensated Chronic Liver Disease. Eur Radiol 2018; 28:3513–3521 [PubMed: 29488082]
69. Yasui Y, Abe T, Kurosaki M, et al. Non-invasive liver fibrosis assessment correlates with collagen and elastic fiber quantity in patients with hepatitis C virus infection. Hepatol Res 2019; 49:33–41 [PubMed: 30419152]
70. Ichikawa S, Motosugi U, Enomoto N, Onishi H. Magnetic resonance elastography can predict development of hepatocellular carcinoma with longitudinally acquired two-point data. Eur Radiol 2019; 29:1013–1021 [PubMed: 30043162]
71. Cho HJ, Kim B, Kim HJ, et al. Liver stiffness measured by MR elastography is a predictor of early HCC recurrence after treatment. Eur Radiol 2020.
72. Wang J, Shan Q, Liu Y, et al. 3D MR Elastography of Hepatocellular Carcinomas as a Potential Biomarker for Predicting Tumor Recurrence. J Magn Reson Imaging 2019; 49:719–730 [PubMed: 30260529]
73. Talwalkar JA, Yin M, Venkatesh S, et al. Feasibility of in vivo MR elastographic splenic stiffness measurements in the assessment of portal hypertension. AJR Am J Roentgenol 2009; 193:122–127 [PubMed: 19542403]
74. Morisaka H, Motosugi U, Ichikawa S, Sano K, Ichikawa T, Enomoto N. Association of splenic MR elastographic findings with gastroesophageal varices in patients with chronic liver disease. J Magn Reson Imaging 2015; 41:117–124 [PubMed: 24243628]
75. Sun HY, Lee JM, Han JK, Choi BI. Usefulness of MR elastography for predicting esophageal varices in cirrhotic patients. J Magn Reson Imaging 2014; 39:559–566 [PubMed: 24115368]
76. Abe H, Midorikawa Y, Matsumoto N, et al. Prediction of esophageal varices by liver and spleen MR elastography. Eur Radiol 2019; 29:6611–6619 [PubMed: 31041563]
77. Wagner M, Hectors S, Bane O, et al. Noninvasive prediction of portal pressure with MR elastography and DCE-MRI of the liver and spleen: Preliminary results. J Magn Reson Imaging 2018
78. Ronot M, Lambert S, Elkrief L, et al. Assessment of portal hypertension and high-risk oesophageal varices with liver and spleen three-dimensional multifrequency MR elastography in liver cirrhosis. Eur Radiol 2014; 24:1394–1402 [PubMed: 24626745]
79. Asrani SK, Talwalkar JA, Kamath PS, et al. Role of Magnetic Resonance Elastography in compensated and decompensated liver disease. Journal of hepatology 2014; 60:934–939 [PubMed: 24362072]
80. Younossi ZM, Stepanova M, Younossi Y, et al. Epidemiology of chronic liver diseases in the USA in the past three decades. Gut 2020; 69:564–568 [PubMed: 31366455]
81. Bedossa P Pathology of non-alcoholic fatty liver disease. Liver Int 2017; 37 Suppl 1:85–89 [PubMed: 28052629]
82. Younossi ZM, Stepanova M, Rafiq N, et al. Nonalcoholic steatofibrosis independently predicts mortality in nonalcoholic fatty liver disease. Hepatol Commun 2017; 1:421–428 [PubMed: 29404470]
83. Cui J, Ang B, Haufe W, et al. Comparative diagnostic accuracy of magnetic resonance elastography vs. eight clinical prediction rules for non-invasive diagnosis of advanced fibrosis in biopsy-proven non-alcoholic fatty liver disease: a prospective study. Aliment Pharmacol Ther 2015; 41:1271–1280 [PubMed: 25873207]
84. Serai SD, Dillman JR, Trout AT. Spin-echo Echo-planar Imaging MR Elastography versus Gradient-echo MR Elastography for Assessment of Liver Stiffness in Children and Young Adults Suspected of Having Liver Disease. Radiology 2017; 282:761–770 [PubMed: 27715486]

85. Trout AT, Sheridan RM, Serai SD, et al. Diagnostic Performance of MR Elastography for Liver Fibrosis in Children and Young Adults with a Spectrum of Liver Diseases. Radiology 2018:172099

86. Wallihan DB, Podberesky DJ, Marino BS, Sticka JS, Serai S. Relationship of MR elastography determined liver stiffness with cardiac function after Fontan palliation. Journal of Magnetic Resonance Imaging 2014; 40:1328–1335 [PubMed: 24408379]

87. Joshi M, Dillman JR, Towbin AJ, Serai SD, Trout AT. MR elastography: high rate of technical success in pediatric and young adult patients. Pediatr Radiol 2017; 47:838–843 [PubMed: 28367603]

88. Etchell E, Jugé L, Hatt A, Sinkus R, Bilston LE. Liver Stiffness Values Are Lower in Pediatric Subjects than in Adults and Increase with Age: A Multifrequency MR Elastography Study. Radiology 2017; 283:222–230 [PubMed: 27755913]

89. Sawh MC, Newton KP, Goyal NP, et al. Normal range for MR elastography measured liver stiffness in children without liver disease. J Magn Reson Imaging 2020; 51:919–927 [PubMed: 31452280]

90. Navin PJ, Olson MC, Knudsen JM, Venkatesh SK. Elastography in the evaluation of liver allograft. Abdom Radiol (NY) 2020;

91. El-Meteini M, Sakr M, Eldorry A, et al. Non-Invasive Assessment of Graft Fibrosis After Living Donor Liver Transplantation: Is There Still a Role for Liver Biopsy? Transplant Proc 2019; 51:2451–2456 [PubMed: 31358454]

92. Lee VS, Miller FH, Omary RA, et al. Magnetic resonance elastography and biomarkers to assess fibrosis from recurrent hepatitis C in liver transplant recipients. Transplantation 2011; 92:581–586 [PubMed: 21822174]

93. Singh S, Venkates SK, Keaveny A, et al. Diagnostic accuracy of magnetic resonance elastography in liver transplant recipients: A pooled analysis. Ann Hepatol 2016; 15:363–376 [PubMed: 27049490]

94. Chen JSD, Glaser K, Yin M. Ergonomic Flexible Drivers for Hepatic MR Elastography. In: ISMRM. Stockholm, Sweden, 2010

95. Wang K, Manning P, Szeverenyi N, et al. Repeatability and reproducibility of 2D and 3D hepatic MR elastography with rigid and flexible drivers at end-expiration and end-inspiration in healthy volunteers. Abdom Radiol (NY) 2017; 42:2843–2854 [PubMed: 28612163]

96. Morin CE, Dillman JR, Serai SD, Trout AT, Tkach JA, Wang H. Comparison of Standard Breath-Held, Free-Breathing, and Compressed Sensing 2D Gradient-Recalled Echo MR Elastography Techniques for Evaluating Liver Stiffness. AJR Am J Roentgenol 2018; 211:W279–W287 [PubMed: 30300003]

97. Murphy IG, Graves MJ, Reid S, et al. Comparison of breath-hold, respiratory navigated and free-breathing MR elastography of the liver. Magn Reson Imaging 2017; 37:46–50 [PubMed: 27746391]

98. Glaser KCJ, Ehman R Fast 2D hepatic MR elastography for free-breathing and short breath hold applications. In: ISMRM. Toronto, Ontario, Canada, 2015

99. Jiahui Li BD, Glaser Kevin J., Yin Ziying, Chen Jun, Alina Allen, Venkatesh Sudhakar K., Armando Manduca, Shah Vijay, Ehman Richard L., Yin Meng. Repeatability and Clinical Performance of Non-gated, Free-breathing, MR Elastography (MRE) of the Liver. In: ISMRM. Montreal, Canada, 2019

100. Ziying Yin BD, Jiahui Li, Glaser Kevin J., Venkatesh Sudhakar K., Manduca Armando, Ehman Richard L., Meng Yin. A Feasibility Study of Nonlinear Mechanical Response Assessment of the Liver with MR Elastography (MRE). In: ISMRM. Paris, France 2018

101. Wagner M, Besa C, Bou Ayache J, et al. Magnetic Resonance Elastography of the Liver: Qualitative and Quantitative Comparison of Gradient Echo and Spin Echo Echoplanar Imaging Sequences. Investigative radiology 2016; 51:575–581 [PubMed: 26982699]

102. Wang J, Glaser KJ, Zhang T, et al. Assessment of advanced hepatic MR elastography methods for susceptibility artifact suppression in clinical patients. J Magn Reson Imaging 2018; 47:976–987 [PubMed: 28801939]

103. Kim YS, Jang YN, Song JS. Comparison of gradient-recalled echo and spin-echo echo-planar imaging MR elastography in staging liver fibrosis: a meta-analysis. Eur Radiol 2018; 28:1709–1718 [PubMed: 29164384]
104. Morisaka H, Motosugi U, Glaser KJ, et al. Comparison of diagnostic accuracies of two- and three-dimensional MR elastography of the liver. J Magn Reson Imaging 2017; 45:1163–1170 [PubMed: 27662640]
105. Asbach P, Klatt D, Hamhaber U, et al. Assessment of liver viscoelasticity using multifrequency MR elastography. Magn Reson Med 2008; 60:373–379 [PubMed: 18666132]
106. Catheline S, Gennisson JL, Delon G, et al. Measuring of viscoelastic properties of homogeneous soft solid using transient elastography: an inverse problem approach. The Journal of the Acoustical Society of America 2004; 116:3734–3741 [PubMed: 15658723]
107. Guo J, Posnansky O, Hirsch S, et al. Fractal network dimension and viscoelastic powerlaw behavior: II. An experimental study of structure-mimicking phantoms by magnetic resonance elastography. Phys Med Biol 2012; 57:4041–4053 [PubMed: 22674199]
108. Klatt D, Friedrich C, Korth Y, Vogt R, Braun J, Sack I. Viscoelastic properties of liver measured by oscillatory rheometry and multifrequency magnetic resonance elastography. Biorheology 2010; 47:133–141 [PubMed: 20683156]
109. Vappou J, Maleke C, Konofagou EE. Quantitative viscoelastic parameters measured by harmonic motion imaging. Phys Med Biol 2009; 54:3579–3594 [PubMed: 19454785]
110. Doyley MM. Model-based elastography: a survey of approaches to the inverse elasticity problem. Phys Med Biol 2012; 57:R35–73 [PubMed: 22222839]
111. Sack I, Beierbach B, Wuerfel J, et al. The impact of aging and gender on brain viscoelasticity. Neuroimage 2009; 46:652–657 [PubMed: 19281851]
112. Suki B, Barabasi AL, Lutchen KR. Lung tissue viscoelasticity: a mathematical framework and its molecular basis. J Appl Physiol (1985) 1994; 76:2749–2759 [PubMed: 7928910]
113. Robert B, Sinkus R, Larrat B, Tanter M, Fink M. A New Rheological Model Based on Fractional Derivatives for Biological Tissues. In: IEEE Ultrasonics Symposium, 2006:1033–1036
114. Klatt D, Hamhaber U, Asbach P, Braun J, Sack I. Noninvasive assessment of the rheological behavior of human organs using multifrequency MR elastography: a study of brain and liver viscoelasticity. Phys Med Biol 2007; 52:7281–7294 [PubMed: 18065839]
115. Barry CT, Mills B, Hah Z, et al. Shear wave dispersion measures liver steatosis. Ultrasound Med Biol 2012; 38:175–182 [PubMed: 22178165]
116. Yin M, Glaser KJ, Manduca A, et al. Distinguishing between Hepatic Inflammation and Fibrosis with MR Elastography. Radiology 2017:160622
117. Yin Z, Glaser KJ, Manduca A, et al. Slip Interface Imaging Predicts Tumor-Brain Adhesion in Vestibular Schwannomas. Radiology 2015; 277:507–517 [PubMed: 26247776]
118. Allen AM, Shah VH, Therneau TM, et al. The Role of Three-Dimensional Magnetic Resonance Elastography in the Diagnosis of Nonalcoholic Steatohepatitis in Obese Patients Undergoing Bariatric Surgery. Hepatology (Baltimore, Md) 2018;
119. Allen AM, Shah VH, Therneau TM, et al. Multiparametric Magnetic Resonance Elastography Improves the Detection of NASH Regression Following Bariatric Surgery. Hepatol Commun 2020; 4:185–192 [PubMed: 32025604]
120. Dzyubak B, Venkatesh SK, Manduca A, Glaser KJ, Ehman RL. Automated liver elasticity calculation for MR elastography. Journal of magnetic resonance imaging : JMRI 2015;
121. Dzyubak B, Glaser KJ, Manduca A, Ehman RL. Automated Liver Elasticity Calculation for 3D MRE. Proceedings of SPIE--the International Society for Optical Engineering 2017; 10134
122. Murphy MC, Manduca A, Trzasko JD, Glaser KJ, Huston J, Ehman RL. Artificial neural networks for stiffness estimation in magnetic resonance elastography. Magn Reson Med 2018; 80:351–360 [PubMed: 29193306]
123. Serai SD, Wallihan DB, Venkatesh SK, et al. Magnetic resonance elastography of the liver in patients status-post fontan procedure: feasibility and preliminary results. Congenit Heart Dis 2014; 9:7–14 [PubMed: 24134059]

124. Poterucha JT, Johnson JN, Qureshi MY, et al. Magnetic Resonance Elastography: A Novel Technique for the Detection of Hepatic Fibrosis and Hepatocellular Carcinoma After the Fontan Operation. Mayo Clin Proc 2015; 90:882–894 [PubMed: 26059757]
125. Poterucha JT, Venkatesh SK, Novak JL, Cetta F. Liver Nodules after the Fontan Operation: Role of Magnetic Resonance Elastography. Tex Heart Inst J 2015; 42:389–392 [PubMed: 26413026]
126. Sugimoto M, Oka H, Kajihama A, et al. Non-invasive assessment of liver fibrosis by magnetic resonance elastography in patients with congenital heart disease undergoing the Fontan procedure and intracardiac repair. J Cardiol 2016; 68:202–208 [PubMed: 27381938]
127. Silva-Sepulveda JA, Fonseca Y, Vodkin I, et al. Evaluation of Fontan liver disease: Correlation of transjugular liver biopsy with magnetic resonance and hemodynamics. Congenit Heart Dis 2019; 14:600–608 [PubMed: 31038848]
128. Egbe A, Miranda WR, Connolly HM, et al. Temporal changes in liver stiffness after Fontan operation: Results of serial magnetic resonance elastography. Int J Cardiol 2018; 258:299–304 [PubMed: 29433966]
129. Alsaied T, Possner M, Lubert AM, et al. Relation of Magnetic Resonance Elastography to Fontan Failure and Portal Hypertension. Am J Cardiol 2019; 124:1454–1459 [PubMed: 31474329]
130. Venkatesh SK, Hoodeshenas S, Venkatesh SH, et al. Magnetic Resonance Elastography of Liver in Light Chain Amyloidosis. J Clin Med 2019; 8
131. Bohte AE, van Dussen L, Akkerman EM, et al. Liver fibrosis in type I Gaucher disease: magnetic resonance imaging, transient elastography and parameters of iron storage. PLoS ONE 2013; 8:e57507 [PubMed: 23554863]
132. Serai SD, Naidu AP, Andrew Burrow T, Prada CE, Xanthakos S, Towbin AJ. Correlating liver stiffness with disease severity scoring system (DS3) values in Gaucher disease type 1 (GD1) patients. Mol Genet Metab 2018; 123:357–363 [PubMed: 29361370]
133. Navin PJ, Gidener T, Allen AM, et al. The Role of Magnetic Resonance Elastography in the Diagnosis of Noncirrhotic Portal Hypertension. Clinical gastroenterology and hepatology : the official clinical practice journal of the American Gastroenterological Association 2019;
134. Navin PJ, Hilscher MB, Welle CL, et al. The Utility of MR Elastography to Differentiate Nodular Regenerative Hyperplasia from Cirrhosis. Hepatology (Baltimore, Md) 2019; 69:452–454
135. Cannella R, Minervini MI, Rachakonda V, Bollino G, Furlan A. Liver stiffness measurement in patients with nodular regenerative hyperplasia undergoing magnetic resonance elastography. Abdom Radiol (NY) 2020; 45:373–383 [PubMed: 31834457]
136. Cui J, Philo L, Nguyen P, et al. Sitagliptin vs. placebo for non-alcoholic fatty liver disease: A randomized controlled trial. J Hepatol 2016; 65:369–376 [PubMed: 27151177]
137. Jayakumar S, Middleton MS, Lawitz EJ, et al. Longitudinal correlations between MRE, MRI-PDFF, and liver histology in patients with non-alcoholic steatohepatitis: Analysis of data from a phase II trial of selonsertib. J Hepatol 2019; 70:133–141 [PubMed: 30291868]
138. Ajmera VH, Cachay E, Ramers C, et al. MRI Assessment of Treatment Response in HIV-associated NAFLD: A Randomized Trial of a Stearoyl-Coenzyme-A-Desaturase-1 Inhibitor (ARRIVE Trial). Hepatology (Baltimore, Md) 2019; 70:1531–1545
139. Harrison SA, Dennis A, Fiore MM, et al. Utility and variability of three non-invasive liver fibrosis imaging modalities to evaluate efficacy of GR-MD-02 in subjects with NASH and bridging fibrosis during a phase-2 randomized clinical trial. PLoS One 2018; 13:e0203054 [PubMed: 30192782]
140. Lee DH, Lee JM, Yi NJ, et al. Hepatic stiffness measurement by using MR elastography: prognostic values after hepatic resection for hepatocellular carcinoma. Eur Radiol 2017; 27:1713–1721 [PubMed: 27456966]
141. Ichikawa S, Motosugi U, Oguri M, Onishi H. Magnetic resonance elastography for prediction of radiation-induced liver disease after stereotactic body radiation therapy. Hepatology (Baltimore, Md) 2017; 66:664–665

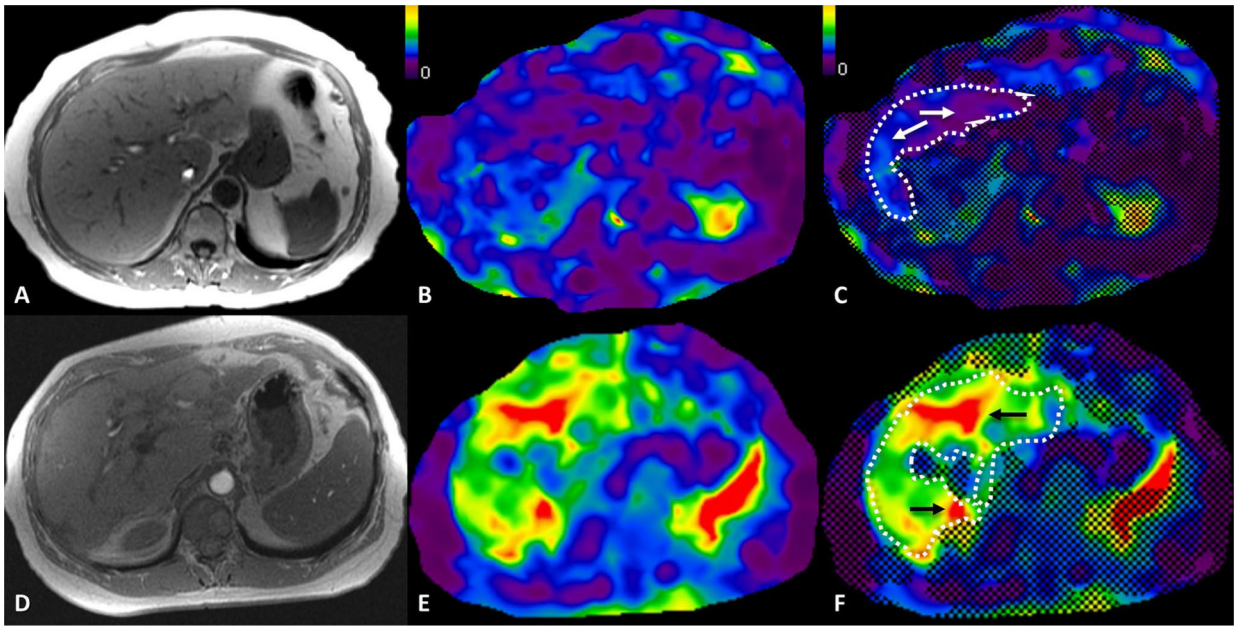

Fig. 1.

LSM measurement. Examples of NAFLD with simple steatosis only (top row) and primary sclerosing cholangitis (bottom row). T1W images (**a**, **d**), color stiffness maps with 0 to 8 kPa scale (**b**, **e**), and with confidence map overlayed (**c**, **f**). The dotted outline represents the free-hand ROIs draw within the confidence map and including most the liver parenchyma. Note there are regions of different stiffness (white arrows in (**c**) and black arrows in (**f**)) particularly in advanced fibrosis and should always be included within the ROI to perform evaluation of liver fibrosis burden. ROI should exclude artifacts and drawn within the confidence maps

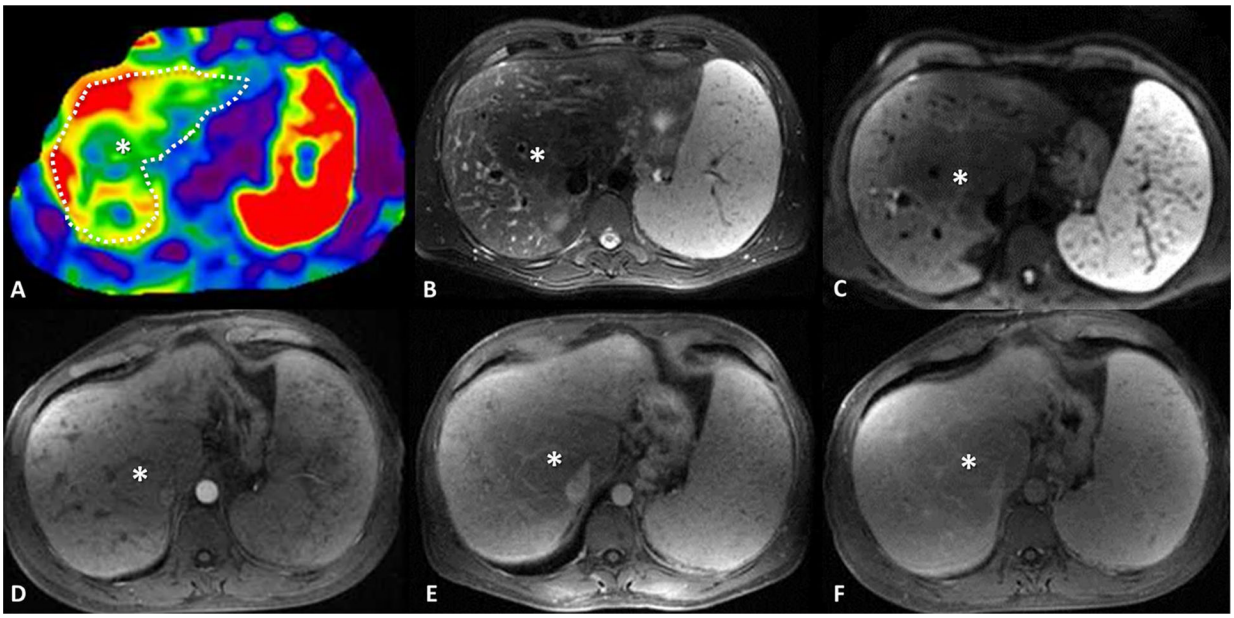

Fig. 2.

MRE in primary sclerosing cholangitis. MRE stiffness map (**a**) with corresponding level T2W (**b**), DWI (**c**), arterial phase (**d**), portal venous phase (**e**) and delayed phase (**f**) images showing heterogeneous stiffness in the liver with a large central macroregenerative nodule (*) which has lower stiffness compared to the peripheral fibrotic liver. The ROI (dotted white line, **a**) for LSM as shown should include macrore-generative nodule for assessment of overall liver fibrosis burden

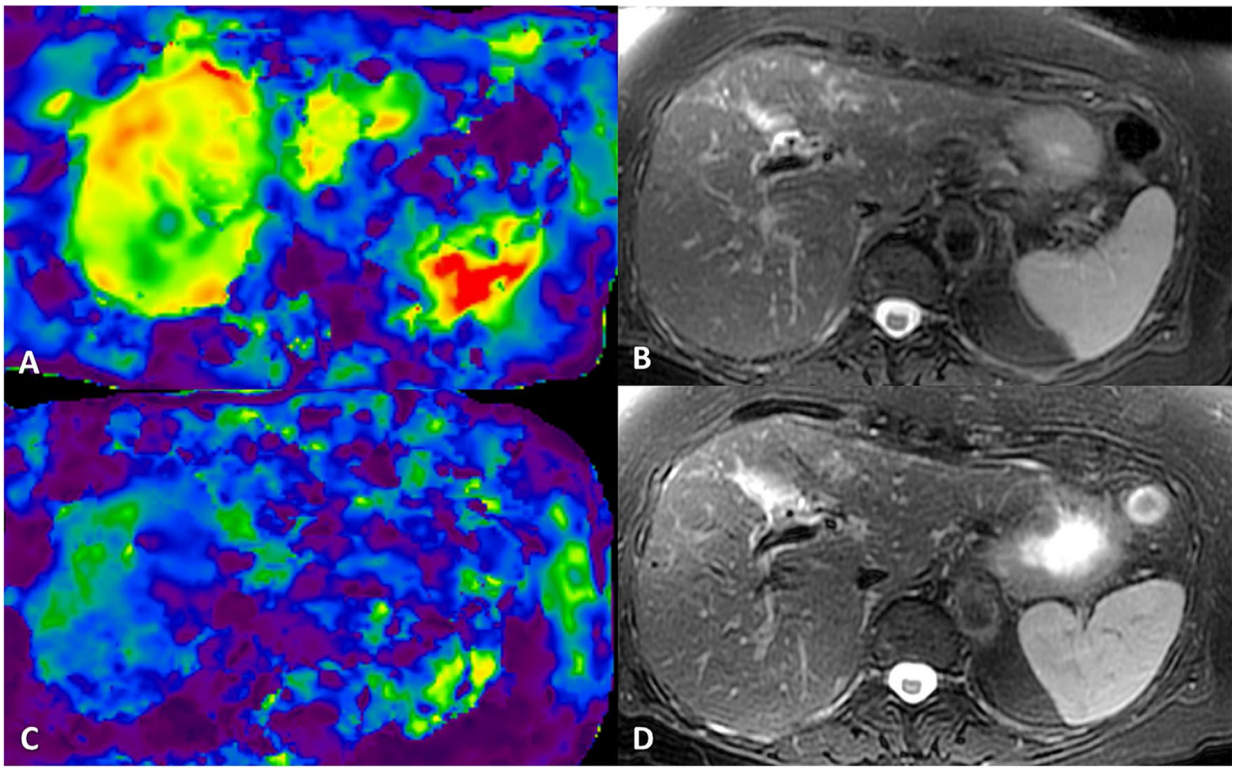

Fig. 3.

MRE of liver before and after antiviral treatment for chronic hepatitis C. Baseline (top row) and follow up (bottom row) stiffness maps (**a**, **c**) and T2W images (**b**, **d**) at similar levels. Baseline stiffness was 6.2 kPa and follow up stiffness was 2.6 kPa. Note there are no significant changes in the morphology of the liver on the T2W images

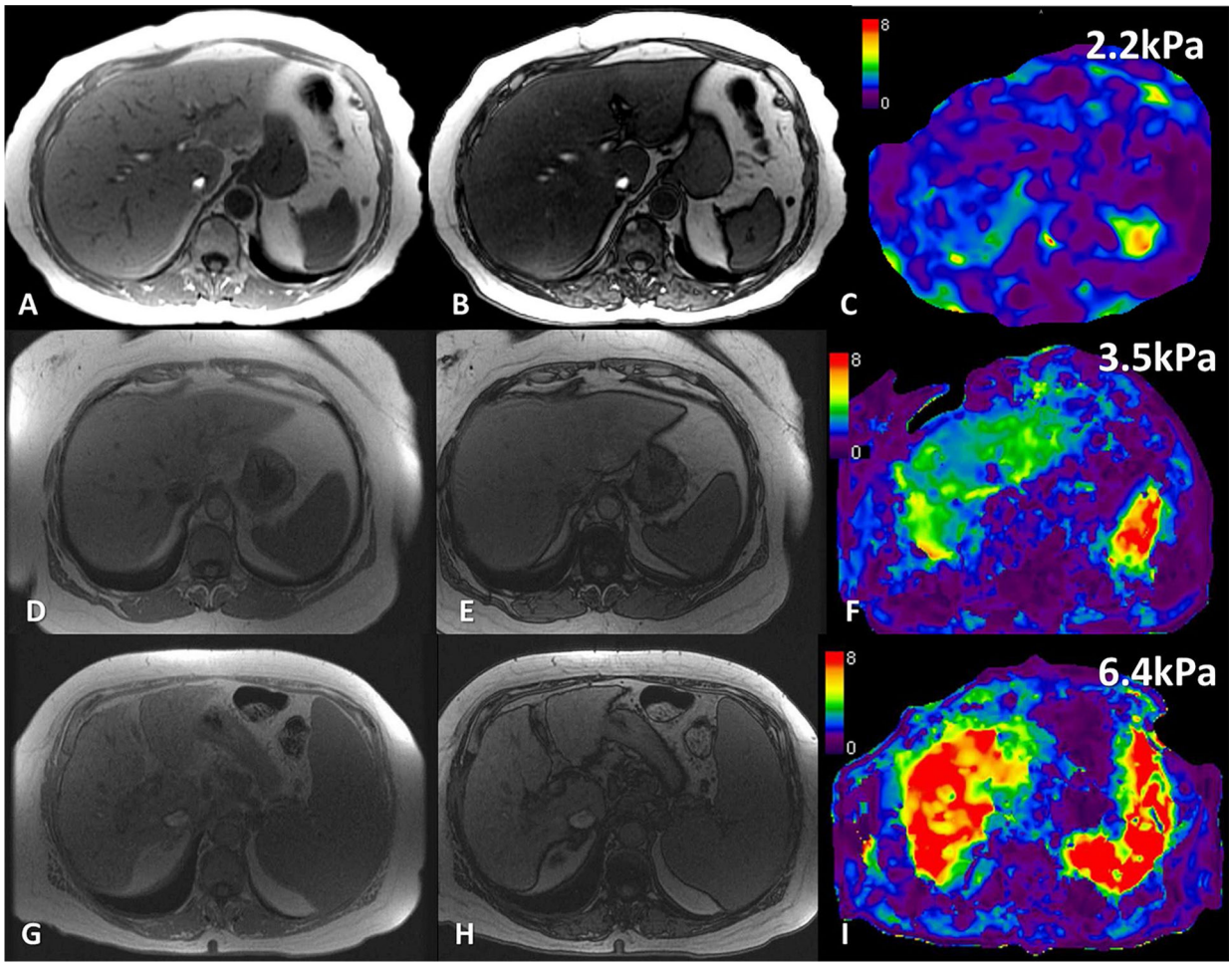

Fig. 4.

Examples of simple steatosis (top row), nonalcoholic steatohepatitis (NASH, middle row) and NASH with cirrhosis (bottom row). In phase images (**a**, **d**, **g**) and opposed phase images (**b**, **e**, **h**) and color stiffness maps (**c**, **f**, **1**) with 0 to 8 kPa scale. NASH causes increased stiffness in the liver compared to simple steatosis alone. NASH with cirrhosis has much higher stiffness compared with NASH alone

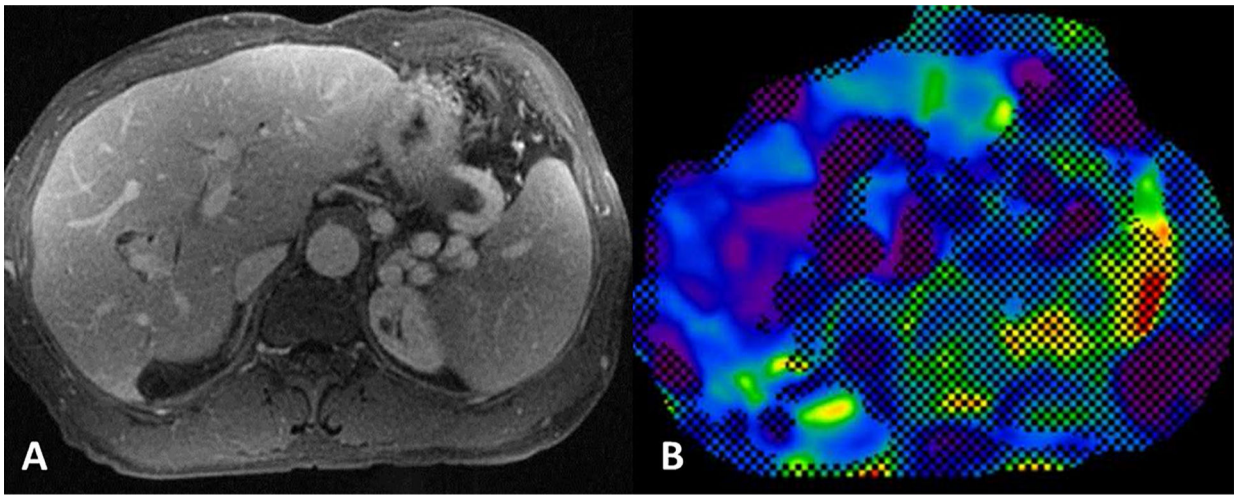

Fig. 5.

MRE of liver graft. Transplantation done for chronic hepatitis C cirrhosis and decompensation. Portal venous phase T1W image (**a**) and stiffness map (**b**) at same level. The graft has normal liver stiffness of 2.1 kPa at 18 months post transplantation. Note splenomegaly and varices due to portal hypertension prior to the transplantation

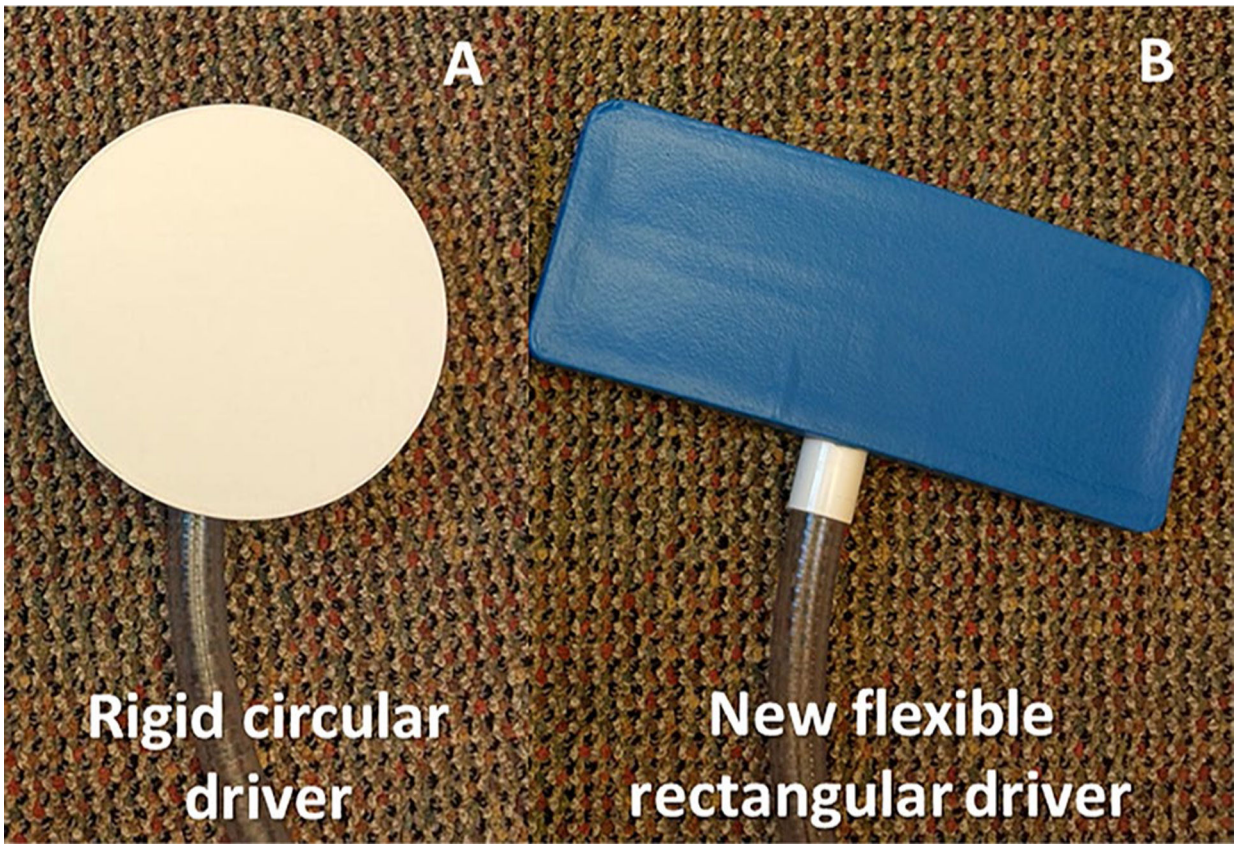

Fig. 6.

Photograph showing the standard rigid circular driver with a vibrating diaphragm (**a**) and new flexible rectangular soft driver (**b**) which is wider than the standard driver

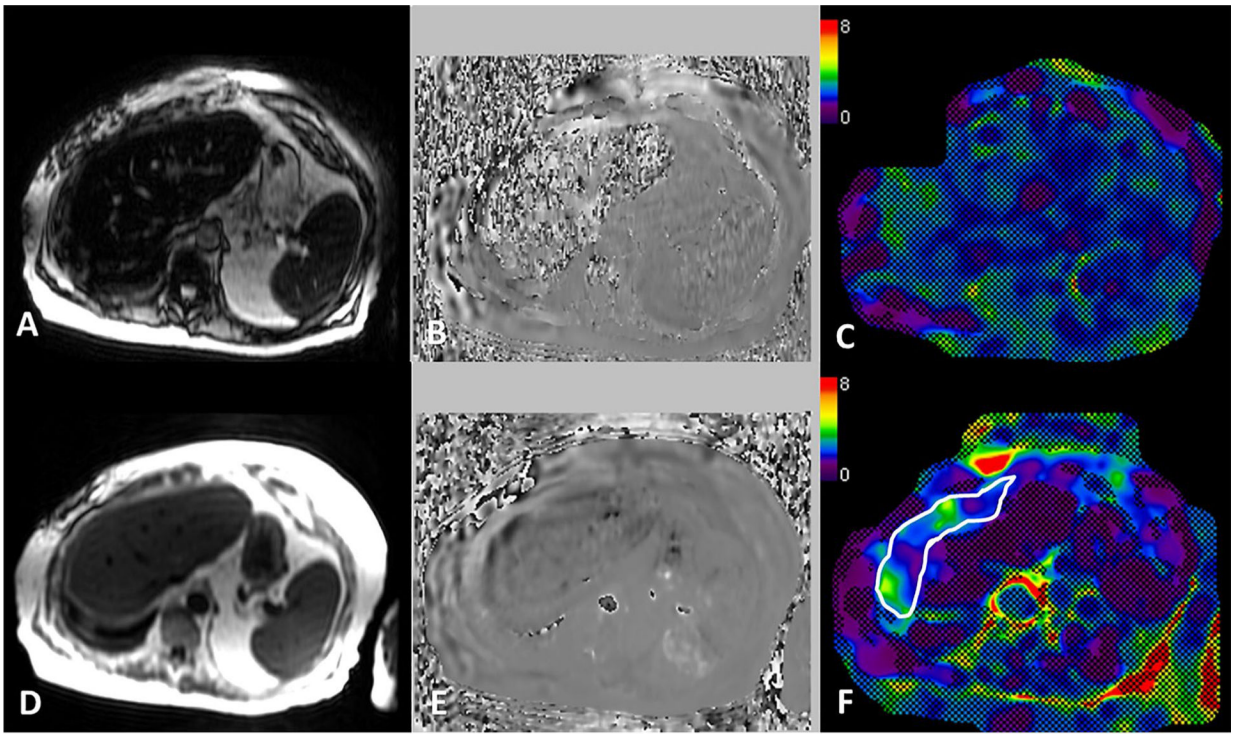

Fig. 7.

MRE in a patient with mild to moderate liver iron overload. Top row images are from 2D-GRE MRE sequence and bottom row images are from SE-EPIMRE sequence. The liver appears hypointense on magnitude image (**a**) with no visible shear waves on phase contrast image (**b**) and confidence map completely masks out the entire abdomen on the stiffness map ©. Magnitude image (**d**) shows better signal in liver parenchyma, shear waves are visible on the phase contras t image (**e**) and LSM is measurable with significant region of liver uncovered on the stiffness map (**f**)

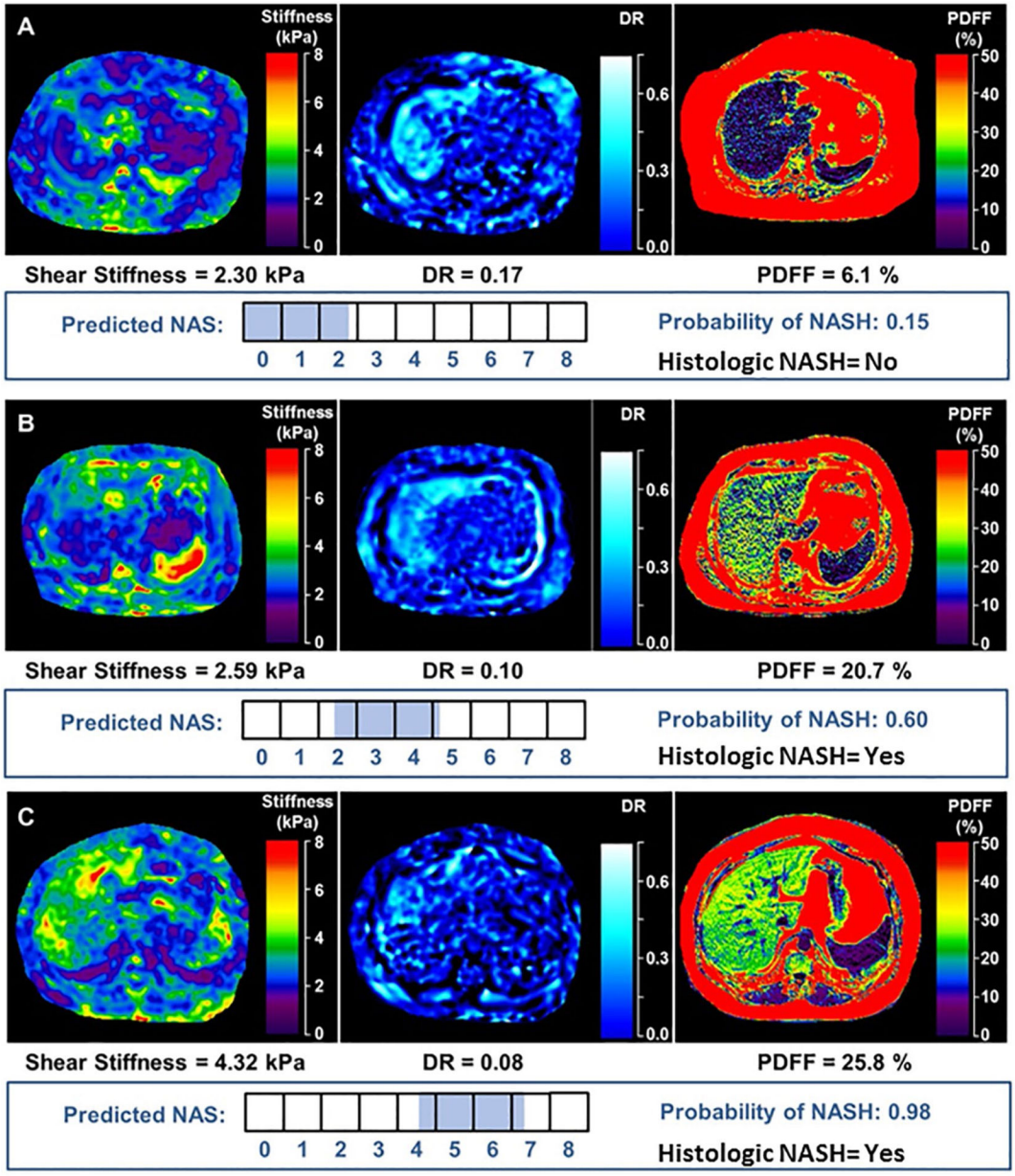

Fig. 8.

Examples of imaging analyses and predicted probabilities of NASH and NAS from 3 study patients. The three imaging parameters included in the predictive model are multifrequency 3D-MRE (mf 3D-MRE) depiction of shear stiffness, damping ratio (DR), and MRI-PDFF depiction of fat fraction. The horizontal boxes illustrate the NAS values ranging from 0 to 8. The shaded part of the boxes represents the predicted range of NAS, which were derived from the regression model as the highest probabilities within the 68% CI. In patient A, who by histology does not have NASH and whose NAS = 0, the logistic regression model using imaging parameters predicted a 15% probability of NASH and a predicted NAS = 0–1. Patient B, with histologic NASH and NAS = 3, has a predicted probability of 60% for NASH and a predicted NAS = 3–4. Finally, patient C, with histologic NASH and NAS = 6,

has a 98% predicted probability of NASH and a predicted NAS = 5–6. (Reproduced with permission from reference [114])

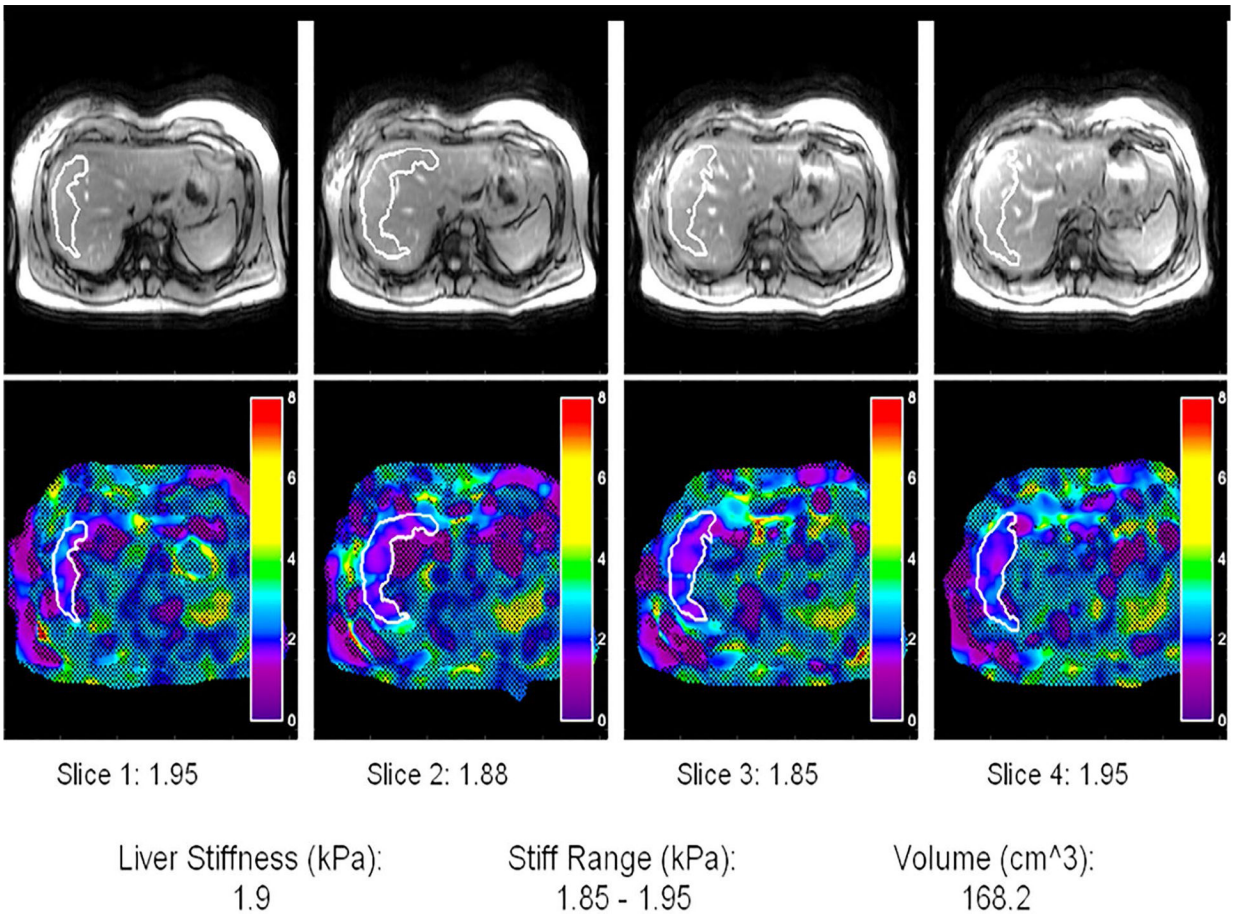

Fig. 9.

Output from automated liver elasticity calculation (ALEC) in a patient normal liver stiffness. Note the ROIs are drawn in the right lobe avoiding liver edges and major vessels. These ROIs are copy pasted automatically on to stiffness map to give the mean stiffness. The stiffness is averaged per pixel. The volume of the liver included in the ROI is also included in the output

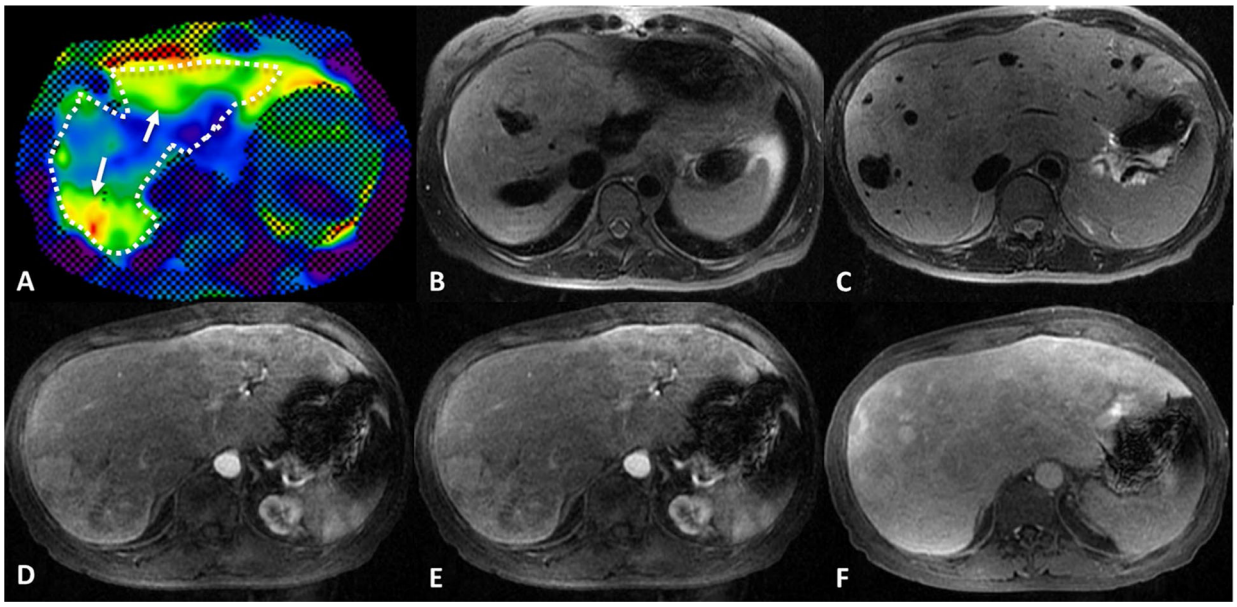

Fig. 10.

MRE in congestive hepatopathy due to Fontan operation for congenital single ventricle. MRE stiffness map (**a**) with T2W (**b**) at higher level and T2W at corresponding level (**c**), arterial phase (**d**), portal venous phase (**e**) and delayed phase (**f**) images showing heterogeneous stiffness distribution in the liver due to congestive hepatopathy. Note the patchy areas of increased stiffness in the periphery (white arrows, **a**) in periphery of the liver parenchyma corresponding to the areas of congestion. The congested areas are seen as areas of early arterial phase enhancement and persistent enhancement in delayed phase. The ROI (white dotted line, **a** for LSM should include these peripheral regions. During follow up similar measurement should be made for consistency and meaningful interpretation of changes

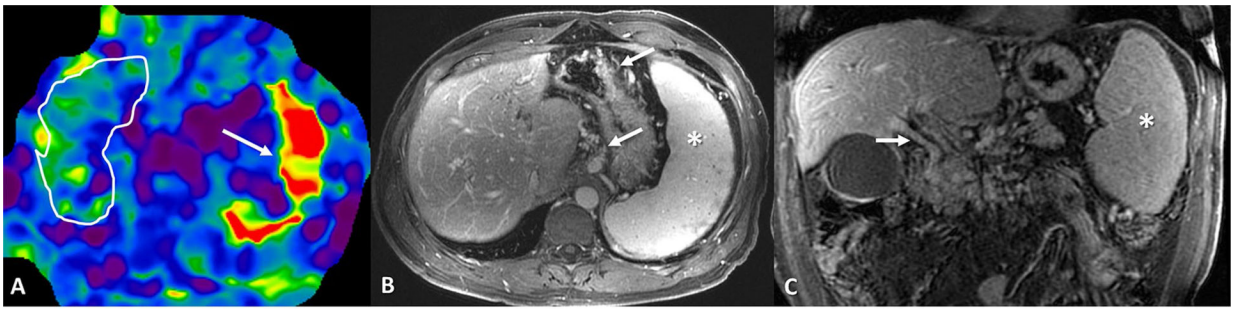

Fig. 11.

Non-cirrhotic portal hypertension (NCPH) due to chronic portal vein thrombosis. MRE stiffness map (**a**), post contrast enhanced portal venous phase axial (**b**) and coronal (**c**) T1W images. There is mildly elevated liver stiffness (**a**) but very stiff spleen (arrow, **a**). Caudate hypertrophy, gastroesophageal and perigastric collaterals (arrows, **b**), pericholedochal collaterals (arrow, **c**) and splenomegaly (*) can be interpreted as cirrhosis with portal hypertension. However, liver stiffness is only mildly elevated to 2.6 kPa. NCPH should always be suspected in patients with mild to moderate liver stiffness but increased spleen stiffness on MRE and signs of portal hypertension on routine liver MRI imaging

Table 1

List of tissue mechanical property terms and their description

Term	Definition/description
Elastography	Medical imaging modality that measures and/or displays mechanical properties of tissues
Stiffness	Qualitative term used to describe the deformation of tissues when subjected to external or internal force. Often interchangeably used with elasticity, bulk modulus, shear modulus and shear stiffness
Shear wave	A wave in which the motion is perpendicular to the direction of mechanical wave propagation. Shear waves are also termed as 'S' wave or secondary wave. The primary wave moves in longitudinal direction of the applied force
Active driver	The main source of mechanical waves for MRE. This is an acoustic driver and consists of ferromagnetic components, and therefore kept outside of magnet room
Passive driver	The non-magnetic device usually made of plastic and kept in contact with patient. This has a drum like membrane which vibrates when acoustic waves are conducted into it from active driver via a plastic tube
Young's elastic modulus (kPa)	The relationship between stress and strain in a material termed as elasticity and applied for uniaxial deformation. This modulus measures elasticity of materials. The modulus is indicative of the tissues ability to resist deformation. Higher the elastic modulus, more elastic is the tissue
Kilopascal (kPa)	Unit of tissues stiffness with elastography. 1 kPa = 1000 Pa (Pa). Pascal is a unit of pressure defined as force per unit area
Shear modulus (G)	Measure of resistance to deformation on application of shear stress. It's a ratio of shear stress to shear strain
Complex shear modulus (G^*)	Measures overall resistance of a material to an applied shear stress. It is composed of two components- the real part or storage modulus (G') and the imaginary or viscous component also known as loss modulus (G'') $G^* = G' + iG''$
Magnitude of the complex shear modulus $\lvert G^* \rvert$	The measured parameter with MRE in kPa units $\lvert G^* \rvert = \sqrt{G'^2 + G''^2}$
Storage modulus	The real part of the complex modulus and describes the tissue resistance to resist stress without loss of energy
Loss modulus	The imaginary part of the complex modulus and describes the energy absorbing behavior of a tissue
Viscoelasticity	Property of material that has both viscosity (absorbing) and elasticity (resistance) behavior. Most biologic tissues have viscoelastic behavior
Attenuation	Loss of amplitude of the waves when propagating through tissues
Damping ratio	$\zeta = G''/(2G')$ Dimensionless quantity that describes how rapidly shear (mechanical) wave decay during propagation in tissues

Table 2

Cut-off MRE LSM values (kPa) for different fibrosis stages for common CLD

CLD etiology	Fibrosis stage ≥ 1	Fibrosis stage ≥ 2	Fibrosis stage ≥ 3	Fibrosis stage ≥ 4	References
Hepatitis B	2.4–2.7	2.7–3.2	3.1–3.7	3.9–5.3	[31,39,40,43]
Hepatitis C	2.3	3.2	4.0	4.6	[32]
NAFLD	2.9–3.1	3.4–3.6	3.6^1.8	4.1–4.7	[10,23,24,47,48]
Alcohol	2.2	2.6	3.3	4	[45]

The values are the range of LSM summarized from the references. The LSM values are rounded off to first decimal point. References are from published series with data available on single etiologies. Meta-analysis including multiple etiologies were excluded when data on single etiologies were not available

CLD chronic liver disease, *kPa* kilopascals

Table 3

Clinically useful LSM cut-offs for classification of broad categories of liver fibrosis stages used at authors institute. These cut-offs are applied to all etiologies of chronic liver disease

LSM cut off	Interpretation
< 2.5 kPa	Normal
2.5 to 3.0 kPa	Normal or inflammation
Increased liver stiffness under appropriate clinical and laboratory findings is compatible with liver fibrosis as below	
3.0 to 3.5 kPa	Stage 1–2 fibrosis
3.5 to 4 kPa	Stage 2–3 fibrosis
4 to 5 kPa	Stage 3–4 fibrosis
> 5 kPa	Stage 4 fibrosis

Abdom Radiol (NY). Author manuscript; available in PMC 2021 March 12.

Table 4

Take Home Points for Clinical Application of Liver MRE

Take Home Points for Clinical Application of Liver MRE
• The mechanical parameter of tissue (stiffness) measured by MRE is the *magnitude of the complex shear modulus*
• The stiffness of liver parenchyma is determined by both composition and organization of the tissue elements (hepatocytes, sinusoids, vessels, extracellular matrix, capsule, etc.), and the physiological (portal pressure, biliary pressure) and pathological processes affecting them
• MRE of liver should ideally be performed in fasting status (at least 3–4 hours). Post-prandial state can cause increased stiffness in patients with fibrosis. Follow up MRE studies should also be performed in fasting status so that changes in LSM can be correctly interpreted
• Sampling larger volumes of liver parenchyma improves accuracy in determining fibrosis burden. Performing the liver MRE with at least four sections through the largest cross-section of liver and also drawing as large as possible regions of interest on stiffness maps would be helpful in obtaining a good sampling of liver parenchyma
• The most common cause of technical failure of the standard GRE-MRE sequence is moderate to severe liver iron overload. The failure is due to “low signal of liver parenchyma” from iron deposition resulting in poor visualization of propagating shear waves. The limitation is not due to failure of propagation of shear waves
• Iron overload in the liver without any associated fibrosis or inflammation is not known to cause increased liver stiffness
• The confounding pathological processes in the evaluation of liver fibrosis using MRE include acute inflammation, congestion, biliary obstruc-tion, and other diffuse infiltrative diseases such as amyloidosis
• LSM should always be interpreted in the given clinical context, and with available liver function tests, and information about liver parenchyma from other MRI sequences when performed with standard MRI liver protocol
• Liver fibrosis staging using MRE LSM cut-offs which differentiates broad categories such as significant fibrosis vs. advanced fibrosis or normal vs. some fibrosis vs. cirrhosis would be most useful for routine clinical practice